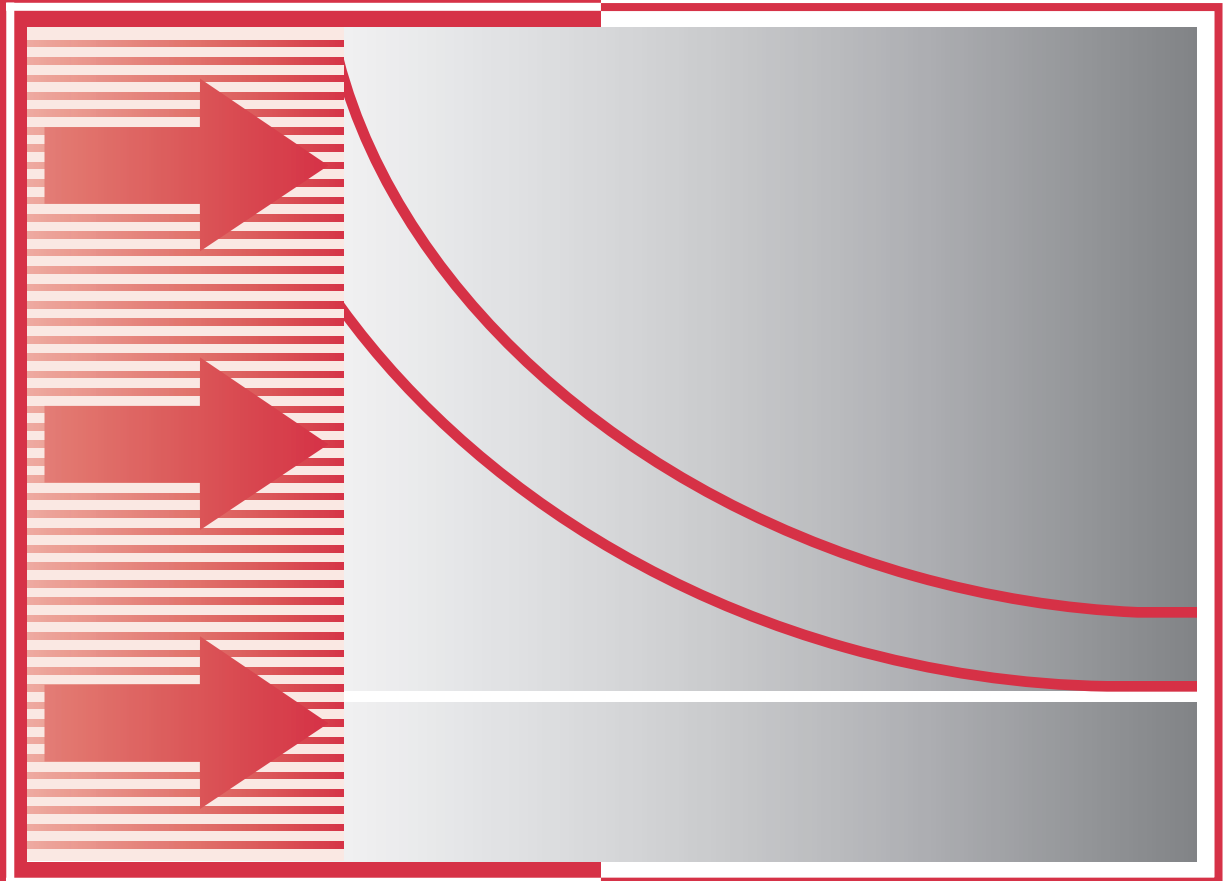


# *CHAPTER* 5

---

## Transient Conduction



**I**n our treatment of conduction we have gradually considered more complicated conditions. We began with the simple case of one-dimensional, steady-state conduction with no internal generation, and we subsequently considered more realistic situations involving multidimensional and generation effects. However, we have not yet considered situations for which conditions change with time.

We now recognize that many heat transfer problems are time dependent. Such *unsteady*, or *transient*, problems typically arise when the boundary conditions of a system are changed. For example, if the surface temperature of a system is altered, the temperature at each point in the system will also begin to change. The changes will continue to occur until a *steady-state* temperature distribution is reached. Consider a hot metal billet that is removed from a furnace and exposed to a cool airstream. Energy is transferred by convection and radiation from its surface to the surroundings. Energy transfer by conduction also occurs from the interior of the metal to the surface, and the temperature at each point in the billet decreases until a steady-state condition is reached. The final properties of the metal will depend significantly on the time-temperature history that results from heat transfer. Controlling the heat transfer is one key to fabricating new materials with enhanced properties.

Our objective in this chapter is to develop procedures for determining the time dependence of the temperature distribution within a solid during a transient process, as well as for determining heat transfer between the solid and its surroundings. The nature of the procedure depends on assumptions that may be made for the process. If, for example, temperature gradients within the solid may be neglected, a comparatively simple approach, termed the *lumped capacitance method*, may be used to determine the variation of temperature with time. The method is developed in Sections 5.1 to 5.3.

Under conditions for which temperature gradients are not negligible, but heat transfer within the solid is one-dimensional, exact solutions to the heat equation may be used to compute the dependence of temperature on both location and time. Such solutions are considered for *finite solids* (plane walls, long cylinders and spheres) in Sections 5.4 to 5.6 and for *semi-infinite solids* in Section 5.7. Section 5.8 presents the transient thermal response of a variety of objects subject to a step change in either surface temperature or surface heat flux. In Section 5.9, the response of a semi-infinite solid to periodic heating conditions at its surface is explored. For more complex conditions, finite-difference or finite-element methods must be used to predict the time dependence of temperatures within the solid, as well as heat rates at its boundaries (Section 5.10).

## 5.1

### The Lumped Capacitance Method

---

A simple, yet common, transient conduction problem is one for which a solid experiences a sudden change in its thermal environment. Consider a hot metal forging that is initially at a uniform temperature  $T_i$  and is quenched by immersing it in a liquid of lower temperature  $T_\infty < T_i$  (Figure 5.1). If the quenching is said to begin at time  $t = 0$ , the temperature of the solid will decrease for time  $t > 0$ , until it eventually

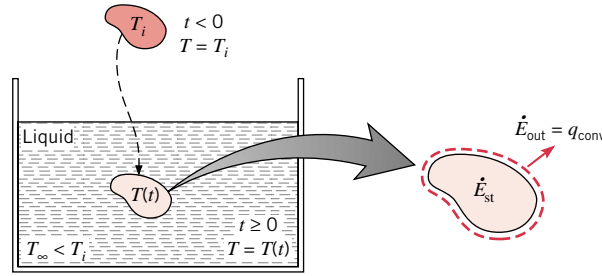


**FIGURE 5.1** Cooling of a hot metal forging.

reaches  $T_\infty$ . This reduction is due to convection heat transfer at the solid–liquid interface. The essence of the lumped capacitance method is the assumption that the temperature of the solid is *spatially uniform* at any instant during the transient process. This assumption implies that temperature gradients within the solid are negligible.

From Fourier’s law, heat conduction in the absence of a temperature gradient implies the existence of infinite thermal conductivity. Such a condition is clearly impossible. However, the condition is closely approximated if the resistance to conduction within the solid is small compared with the resistance to heat transfer between the solid and its surroundings. For now we assume that this is, in fact, the case.

In neglecting temperature gradients within the solid, we can no longer consider the problem from within the framework of the heat equation. Instead, the transient temperature response is determined by formulating an overall energy balance on the solid. This balance must relate the rate of heat loss at the surface to the rate of change of the internal energy. Applying Equation 1.11c to the control volume of Figure 5.1, this requirement takes the form

$$-\dot{E}_{\text{out}} = \dot{E}_{\text{st}} \quad (5.1)$$

or

$$-hA_s(T - T_\infty) = \rho Vc \frac{dT}{dt} \quad (5.2)$$

Introducing the temperature difference

$$\theta \equiv T - T_\infty \quad (5.3)$$

and recognizing that  $(d\theta/dt) = (dT/dt)$  if  $T_\infty$  is constant, it follows that

$$\frac{\rho Vc}{hA_s} \frac{d\theta}{dt} = -\theta$$

Separating variables and integrating from the initial condition, for which  $t = 0$  and  $T(0) = T_i$ , we then obtain

$$\frac{\rho Vc}{hA_s} \int_{\theta_i}^{\theta} \frac{d\theta}{\theta} = - \int_0^t dt$$

where

$$\theta_i \equiv T_i - T_\infty \quad (5.4)$$

Evaluating the integrals, it follows that

$$\frac{\rho V c}{h A_s} \ln \frac{\theta_i}{\theta} = t \quad (5.5)$$

or

$$\frac{\theta}{\theta_i} = \frac{T - T_\infty}{T_i - T_\infty} = \exp \left[ - \left( \frac{h A_s}{\rho V c} \right) t \right] \quad (5.6)$$

Equation 5.5 may be used to determine the time required for the solid to reach some temperature  $T$ , or, conversely, Equation 5.6 may be used to compute the temperature reached by the solid at some time  $t$ .

The foregoing results indicate that the difference between the solid and fluid temperatures must decay exponentially to zero as  $t$  approaches infinity. This behavior is shown in Figure 5.2. From Equation 5.6 it is also evident that the quantity  $(\rho V c / h A_s)$  may be interpreted as a *thermal time constant* expressed as

$$\tau_t = \left( \frac{1}{h A_s} \right) (\rho V c) = R_t C_t \quad (5.7)$$

where  $R_t$  is the resistance to convection heat transfer and  $C_t$  is the *lumped thermal capacitance* of the solid. Any increase in  $R_t$  or  $C_t$  will cause a solid to respond more slowly to changes in its thermal environment. This behavior is analogous to the voltage decay that occurs when a capacitor is discharged through a resistor in an electrical  $RC$  circuit.

To determine the total energy transfer  $Q$  occurring up to some time  $t$ , we simply write

$$Q = \int_0^t q \, dt = h A_s \int_0^t \theta \, dt$$

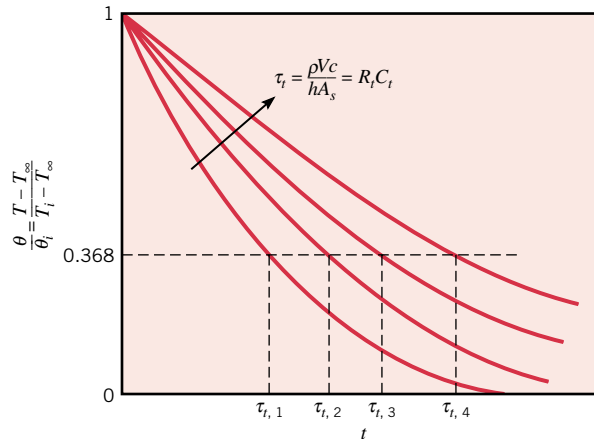


**FIGURE 5.2** Transient temperature response of lumped capacitance solids for different thermal time constants  $\tau_t$ .

Substituting for  $\theta$  from Equation 5.6 and integrating, we obtain

$$Q = (\rho V c) \theta_i \left[ 1 - \exp\left(-\frac{t}{\tau_i}\right) \right] \quad (5.8a)$$

The quantity  $Q$  is, of course, related to the change in the internal energy of the solid, and from Equation 1.11b

$$-Q = \Delta E_{st} \quad (5.8b)$$

For quenching  $Q$  is positive and the solid experiences a decrease in energy. Equations 5.5, 5.6, and 5.8a also apply to situations where the solid is heated ( $\theta < 0$ ), in which case  $Q$  is negative and the internal energy of the solid increases.

## 5.2

### Validity of the Lumped Capacitance Method

From the foregoing results it is easy to see why there is a strong preference for using the lumped capacitance method. It is certainly the simplest and most convenient method that can be used to solve transient heating and cooling problems. Hence it is important to determine under what conditions it may be used with reasonable accuracy.

To develop a suitable criterion consider steady-state conduction through the plane wall of area  $A$  (Figure 5.3). Although we are assuming steady-state conditions, this criterion is readily extended to transient processes. One surface is maintained at a temperature  $T_{s,1}$  and the other surface is exposed to a fluid of temperature  $T_\infty < T_{s,1}$ . The temperature of this surface will be some intermediate value,  $T_{s,2}$ , for which  $T_\infty < T_{s,2} < T_{s,1}$ . Hence under steady-state conditions the surface energy balance, Equation 1.12, reduces to

$$\frac{kA}{L} (T_{s,1} - T_{s,2}) = hA(T_{s,2} - T_\infty)$$

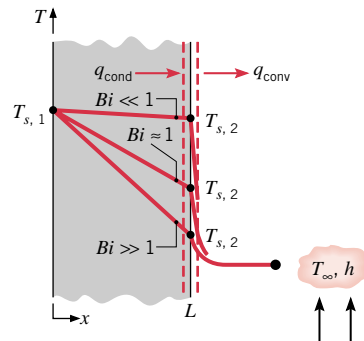


**FIGURE 5.3**

Effect of Biot number on steady-state temperature distribution in a plane wall with surface convection.

where  $k$  is the thermal conductivity of the solid. Rearranging, we then obtain

$$\frac{T_{s,1} - T_{s,2}}{T_{s,2} - T_\infty} = \frac{(L/kA)}{(1/hA)} = \frac{R_{\text{cond}}}{R_{\text{conv}}} = \frac{hL}{k} \equiv Bi \quad (5.9)$$

The quantity  $(hL/k)$  appearing in Equation 5.9 is a *dimensionless parameter*. It is termed the *Biot number*, and it plays a fundamental role in conduction problems that involve surface convection effects. According to Equation 5.9 and as illustrated in Figure 5.3, the Biot number provides a measure of the temperature drop in the solid relative to the temperature difference between the surface and the fluid. Note especially the conditions corresponding to  $Bi \ll 1$ . The results suggest that, for these conditions, it is reasonable to *assume* a uniform temperature distribution within a solid at any time during a transient process. This result may also be associated with interpretation of the Biot number as a ratio of thermal resistances, Equation 5.9. *If  $Bi \ll 1$ , the resistance to conduction within the solid is much less than the resistance to convection across the fluid boundary layer.* Hence the assumption of a uniform temperature distribution is reasonable.

We have introduced the Biot number because of its significance to transient conduction problems. Consider the plane wall of Figure 5.4, which is initially at a uniform temperature  $T_i$  and experiences convection cooling when it is immersed in a fluid of  $T_\infty < T_i$ . The problem may be treated as one-dimensional in  $x$ , and we are interested in the temperature variation with position and time,  $T(x, t)$ . This variation is a strong function of the Biot number, and three conditions are shown in Figure 5.4. For  $Bi \ll 1$  the temperature gradient in the solid is small and  $T(x, t) \approx T(t)$ . Virtually all the temperature difference is between the solid and the fluid, and the solid temperature remains nearly uniform as it decreases to  $T_\infty$ . For moderate to large values of the Biot number, however, the temperature gradients within the solid are significant. Hence  $T = T(x, t)$ . Note that for  $Bi \gg 1$ , the temperature difference across the solid is much larger than that between the surface and the fluid.

We conclude this section by emphasizing the importance of the lumped capacitance method. Its inherent simplicity renders it the preferred method for solving

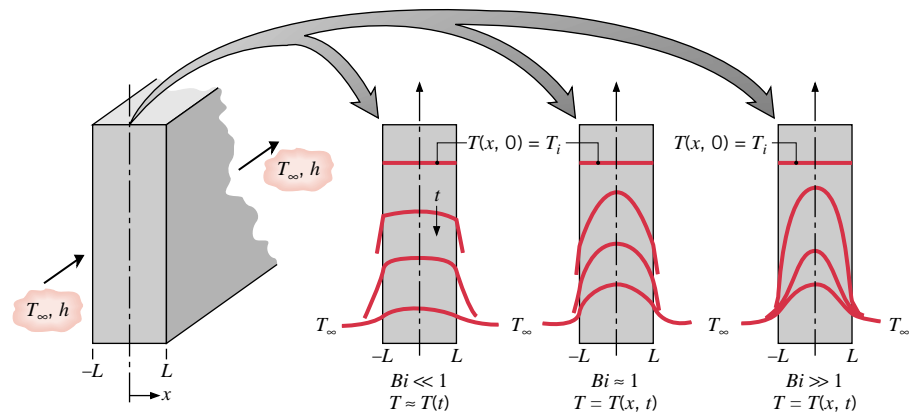


**FIGURE 5.4** Transient temperature distributions for different Biot numbers in a plane wall symmetrically cooled by convection.

transient heating and cooling problems. Hence, when confronted with such a problem, *the very first thing that one should do is calculate the Biot number*. If the following condition is satisfied

$$Bi = \frac{hL_c}{k} < 0.1 \quad (5.10)$$

the error associated with using the lumped capacitance method is small. For convenience, it is customary to define the *characteristic length* of Equation 5.10 as the ratio of the solid's volume to surface area,  $L_c \equiv V/A_s$ . Such a definition facilitates calculation of  $L_c$  for solids of complicated shape and reduces to the half-thickness  $L$  for a plane wall of thickness  $2L$  (Figure 5.4), to  $r_o/2$  for a long cylinder, and to  $r_o/3$  for a sphere. However, if one wishes to implement the criterion in a conservative fashion,  $L_c$  should be associated with the length scale corresponding to the maximum spatial temperature difference. Accordingly, for a symmetrically heated (or cooled) plane wall of thickness  $2L$ ,  $L_c$  would remain equal to the half-thickness  $L$ . However, for a long cylinder or sphere,  $L_c$  would equal the actual radius  $r_o$ , rather than  $r_o/2$  or  $r_o/3$ .

Finally, we note that, with  $L_c \equiv V/A_s$ , the exponent of Equation 5.6 may be expressed as

$$\frac{hA_s t}{\rho V c} = \frac{ht}{\rho c L_c} = \frac{hL_c}{k} \frac{k}{\rho c} \frac{t}{L_c^2} = \frac{hL_c}{k} \frac{\alpha t}{L_c^2}$$

or

$$\frac{hA_s t}{\rho V c} = Bi \cdot Fo \quad (5.11)$$

where

$$Fo \equiv \frac{\alpha t}{L_c^2} \quad (5.12)$$

is termed the Fourier number. It is a *dimensionless time*, which, with the Biot number, characterizes transient conduction problems. Substituting Equation 5.11 into 5.6, we obtain

$$\frac{\theta}{\theta_i} = \frac{T - T_\infty}{T_i - T_\infty} = \exp(-Bi \cdot Fo) \quad (5.13)$$

### EXAMPLE 5.1

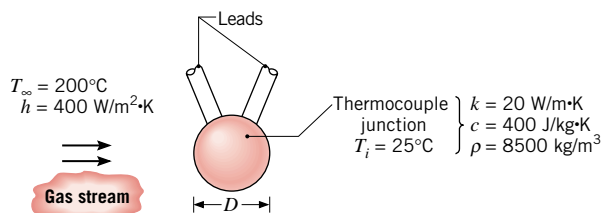
A thermocouple junction, which may be approximated as a sphere, is to be used for temperature measurement in a gas stream. The convection coefficient between the junction surface and the gas is  $h = 400 \text{ W/m}^2 \cdot \text{K}$ , and the junction thermophysical properties are  $k = 20 \text{ W/m} \cdot \text{K}$ ,  $c = 400 \text{ J/kg} \cdot \text{K}$ , and  $\rho = 8500 \text{ kg/m}^3$ . Determine the junction diameter needed for the thermocouple to have a time constant of 1 s. If the junction is at  $25^\circ\text{C}$  and is placed in a gas stream that is at  $200^\circ\text{C}$ , how long will it take for the junction to reach  $199^\circ\text{C}$ ?

**SOLUTION**

**Known:** Thermophysical properties of thermocouple junction used to measure temperature of a gas stream.

**Find:**

1. Junction diameter needed for a time constant of 1 s.
2. Time required to reach 199°C in gas stream at 200°C.

**Schematic:****Assumptions:**

1. Temperature of junction is uniform at any instant.
2. Radiation exchange with the surroundings is negligible.
3. Losses by conduction through the leads are negligible.
4. Constant properties.

**Analysis:**

1. Because the junction diameter is unknown, it is not possible to begin the solution by determining whether the criterion for using the lumped capacitance method, Equation 5.10, is satisfied. However, a reasonable approach is to use the method to find the diameter and to then determine whether the criterion is satisfied. From Equation 5.7 and the fact that  $A_s = \pi D^2$  and  $V = \pi D^3/6$  for a sphere, it follows that

$$\tau_t = \frac{1}{h\pi D^2} \times \frac{\rho\pi D^3}{6} c$$

Rearranging and substituting numerical values,

$$D = \frac{6h\tau_t}{\rho c} = \frac{6 \times 400 \text{ W/m}^2 \cdot \text{K} \times 1 \text{ s}}{8500 \text{ kg/m}^3 \times 400 \text{ J/kg} \cdot \text{K}} = 7.06 \times 10^{-4} \text{ m} \quad \triangleleft$$

With  $L_c = r_o/3$  it then follows from Equation 5.10 that

$$Bi = \frac{h(r_o/3)}{k} = \frac{400 \text{ W/m}^2 \cdot \text{K} \times 3.53 \times 10^{-4} \text{ m}}{3 \times 20 \text{ W/m} \cdot \text{K}} = 2.35 \times 10^{-3}$$

Accordingly, Equation 5.10 is satisfied (for  $L_c = r_o$ , as well as for  $L_c = r_o/3$ ) and the lumped capacitance method may be used to an excellent approximation.



2. From Equation 5.5 the time required for the junction to reach  $T = 199^\circ\text{C}$  is

$$t = \frac{\rho(\pi D^3/6)c}{h(\pi D^2)} \ln \frac{T_i - T_\infty}{T - T_\infty} = \frac{\rho D c}{6h} \ln \frac{T_i - T_\infty}{T - T_\infty}$$

$$t = \frac{8500 \text{ kg/m}^3 \times 7.06 \times 10^{-4} \text{ m} \times 400 \text{ J/kg} \cdot \text{K}}{6 \times 400 \text{ W/m}^2 \cdot \text{K}} \ln \frac{25 - 200}{199 - 200}$$

$$t = 5.2 \text{ s} \approx 5\tau_t$$

**Comments:** Heat transfer due to radiation exchange between the junction and the surroundings and conduction through the leads would affect the time response of the junction and would, in fact, yield an equilibrium temperature that differs from  $T_\infty$ .

## 5.3

### General Lumped Capacitance Analysis

Although transient conduction in a solid is commonly initiated by convection heat transfer to or from an adjoining fluid, other processes may induce transient thermal conditions within the solid. For example, a solid may be separated from large surroundings by a gas or vacuum. If the temperatures of the solid and surroundings differ, radiation exchange could cause the internal thermal energy, and hence the temperature, of the solid to change. Temperature changes could also be induced by applying a heat flux at a portion, or all, of the surface and/or by initiating thermal energy generation within the solid. Surface heating could, for example, be applied by attaching a film or sheet electrical heater to the surface, while thermal energy could be generated by passing an electrical current through the solid.

Figure 5.5 depicts a situation for which thermal conditions within a solid may be influenced simultaneously by convection, radiation, an applied surface heat flux, and internal energy generation. It is presumed that, initially ( $t = 0$ ), the temperature of the solid ( $T_i$ ) differs from that of the fluid,  $T_\infty$ , and the surroundings,  $T_{\text{sur}}$ , and that both surface and volumetric heating ( $q_s''$  and  $\dot{q}$ ) are initiated. The imposed heat flux

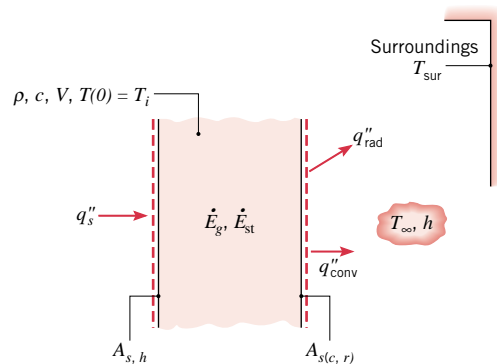


**FIGURE 5.5**

Control surface for general lumped capacitance analysis.

$q_s''$  and the convection–radiation heat transfer occur at mutually exclusive portions of the surface,  $A_{s(h)}$  and  $A_{s(c,r)}$ , respectively, and convection–radiation transfer is presumed to be *from* the surface. Moreover, although convection and radiation have been prescribed for the same surface, the surfaces may, in fact, differ ( $A_{s,c} \neq A_{s,r}$ ). Applying conservation of energy at any instant  $t$ , it follows from Equation 1.11c that

$$q_s'' A_{s,h} + \dot{E}_g - (q_{\text{conv}}'' + q_{\text{rad}}'') A_{s(c,r)} = \rho V c \frac{dT}{dt} \quad (5.14)$$

or, from Equations 1.3a and 1.7,

$$q_s'' A_{s,h} + \dot{E}_g - [h(T - T_\infty) + \varepsilon \sigma (T^4 - T_{\text{sur}}^4)] A_{s(c,r)} = \rho V c \frac{dT}{dt} \quad (5.15)$$

Equation 5.15 is a nonlinear, first-order, nonhomogeneous, ordinary differential equation that cannot be integrated to obtain an exact solution.<sup>1</sup> However, exact solutions may be obtained for simplified versions of the equation. For example, if there is no imposed heat flux or generation and convection is either nonexistent (a vacuum) or negligible relative to radiation, Equation 5.15 reduces to

$$\rho V c \frac{dT}{dt} = -\varepsilon A_{s,r} \sigma (T^4 - T_{\text{sur}}^4) \quad (5.16)$$

Separating variables and integrating from the initial condition to any time  $t$ , it follows that

$$\frac{\varepsilon A_{s,r} \sigma}{\rho V c} \int_0^t dt = \int_{T_i}^T \frac{dT}{T_{\text{sur}}^4 - T^4} \quad (5.17)$$

Evaluating both integrals and rearranging, the time required to reach the temperature  $T$  becomes

$$t = \frac{\rho V c}{4 \varepsilon A_{s,r} \sigma T_{\text{sur}}^3} \left\{ \ln \left| \frac{T_{\text{sur}} + T}{T_{\text{sur}} - T} \right| - \ln \left| \frac{T_{\text{sur}} + T_i}{T_{\text{sur}} - T_i} \right| + 2 \left[ \tan^{-1} \left( \frac{T}{T_{\text{sur}}} \right) - \tan^{-1} \left( \frac{T_i}{T_{\text{sur}}} \right) \right] \right\} \quad (5.18)$$

This expression cannot be used to evaluate  $T$  explicitly in terms of  $t$ ,  $T_i$ , and  $T_{\text{sur}}$ , nor does it readily reduce to the limiting result for  $T_{\text{sur}} = 0$  (radiation to deep space). However, returning to Equation 5.17, its solution for  $T_{\text{sur}} = 0$  yields

$$t = \frac{\rho V c}{3 \varepsilon A_{s,r} \sigma} \left( \frac{1}{T^3} - \frac{1}{T_i^3} \right) \quad (5.19)$$

An exact solution to Equation 5.15 may also be obtained if radiation may be neglected and  $h$  is independent of time. Introducing a temperature difference  $\theta \equiv T - T_\infty$ , where  $d\theta/dt = dT/dt$ , Equation 5.15 reduces to a linear, first-order, nonhomogeneous differential equation of the form

$$\frac{d\theta}{dt} + a\theta - b = 0 \quad (5.20)$$

<sup>1</sup>An approximate, finite-difference solution may be obtained by *discretizing* the time derivative (Section 5.10) and *marching* the solution out in time.

where  $a \equiv (hA_{s,c}/\rho Vc)$  and  $b \equiv [(q_s''A_{s,h} + \dot{E}_g)/\rho Vc]$ . Although Equation 5.20 may be solved by summing its homogeneous and particular solutions, an alternative approach is to eliminate the nonhomogeneity by introducing the transformation

$$\theta' \equiv \theta - \frac{b}{a} \quad (5.21)$$

Recognizing that  $d\theta'/dt = d\theta/dt$ , Equation 5.21 may be substituted into (5.20) to yield

$$\frac{d\theta'}{dt} + a\theta' = 0 \quad (5.22)$$

Separating variables and integrating from 0 to  $t$  ( $\theta'_i$  to  $\theta'$ ), it follows that

$$\frac{\theta'}{\theta'_i} = \exp(-at) \quad (5.23)$$

or substituting for  $\theta'$  and  $\theta$ ,

$$\frac{T - T_\infty - (b/a)}{T_i - T_\infty - (b/a)} = \exp(-at) \quad (5.24)$$

Hence

$$\frac{T - T_\infty}{T_i - T_\infty} = \exp(-at) + \frac{b/a}{T_i - T_\infty} [1 - \exp(-at)] \quad (5.25)$$

As it must, Equation 5.25 reduces to Equation 5.6 when  $b = 0$  and yields  $T = T_i$  at  $t = 0$ . As  $t \rightarrow \infty$ , Equation 5.25 reduces to  $(T - T_\infty) = (b/a)$ , which could also be obtained by performing an energy balance on the control surface of Figure 5.5 for steady-state conditions.

### EXAMPLE 5.2

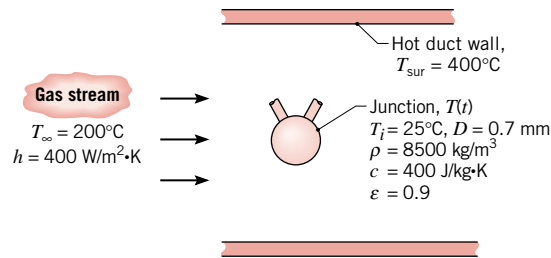
Consider the thermocouple and convection conditions of Example 5.1, but now allow for radiation exchange with the walls of a duct that encloses the gas stream. If the duct walls are at 400°C and the emissivity of the thermocouple bead is 0.9, calculate the steady-state temperature of the junction. Also, determine the time for the junction temperature to increase from an initial condition of 25°C to a temperature that is within 1°C of its steady-state value.

### SOLUTION

**Known:** Thermophysical properties and diameter of the thermocouple junction used to measure temperature of a gas stream passing through a duct with hot walls.

### Find:

1. Steady-state temperature of the junction.
2. Time required for the thermocouple to reach a temperature that is within 1°C of its steady-state value.

**Schematic:**

**Assumptions:** Same as Example 5.1, but radiation transfer is no longer treated as negligible and is approximated as exchange between a small surface and large surroundings.

**Analysis:**

1. For steady-state conditions, the energy balance on the thermocouple junction has the form

$$\dot{E}_{\text{in}} - \dot{E}_{\text{out}} = 0$$

Recognizing that net radiation to the junction must be balanced by convection from the junction to the gas, the energy balance may be expressed as

$$[\epsilon\sigma(T_{\text{sur}}^4 - T^4) - h(T - T_{\infty})]A_s = 0$$

Substituting numerical values, we obtain

$$T = 218.7^{\circ}\text{C} \quad \triangleleft$$

2. The temperature-time history,  $T(t)$ , for the junction, initially at  $T(0) = T_i = 25^{\circ}\text{C}$ , follows from the energy balance for transient conditions,

$$\dot{E}_{\text{in}} - \dot{E}_{\text{out}} = \dot{E}_{\text{st}}$$

From Equation 5.15, the energy balance may be expressed as

$$- [h(T - T_{\infty}) + \epsilon\sigma(T^4 - T_{\text{sur}}^4)]A_s = \rho Vc \frac{dT}{dt}$$

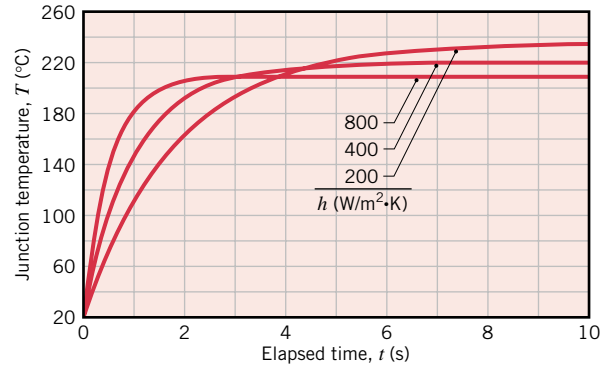
The solution to this first-order differential equation can be obtained by numerical integration, giving the result,  $T(4.9 \text{ s}) = 217.7^{\circ}\text{C}$ . Hence, the time required to reach a temperature that is within  $1^{\circ}\text{C}$  of the steady-state value is

$$t = 4.9 \text{ s.} \quad \triangleleft$$

**Comments:**

1. The effect of radiation exchange with the hot duct walls is to increase the junction temperature, such that the thermocouple indicates an erroneous gas stream temperature that exceeds the actual temperature by  $18.7^{\circ}\text{C}$ . The time required to reach a temperature that is within  $1^{\circ}\text{C}$  of the steady-state value is slightly less than the result of Example 5.1, which only considers convection heat transfer. Why is this so?

2. The response of the thermocouple and the indicated gas stream temperature depend on the velocity of the gas stream, which in turn affects the magnitude of the convection coefficient. Temperature-time histories for the thermocouple junction are shown in the following graph for values of  $h = 200, 400$ , and  $800 \text{ W/m}^2 \cdot \text{K}$ .



The effect of increasing the convection coefficient is to cause the junction to indicate a temperature closer to that of the gas stream. Further, the effect is to reduce the time required for the junction to reach the near-steady-state condition. What physical explanation can you give for these results?

3. The *IHT* software accompanying this text includes an integral function,  $\text{Der}(T, t)$ , that can be used to represent the temperature-time derivative and to integrate first-order differential equations. For this problem, an energy balance relation of the following form may be entered into the *Workspace*,

$$(-h(T - T_{\text{inf}}) - \epsilon \sigma (T^4 - T_{\text{sur}}^4)) A_s = \rho V c \text{Der}(T, t)$$

After hitting the *Solve* button, the *Diff/Integral Equations* pad will appear, identifying the independent variable  $t$  and providing boxes (*Start*, *Stop*, and *Step*) for entering the integration limits and the time increment  $\Delta t$ , respectively, as well as the initial condition (*IC*). Alternatively, the *IHT Lumped Capacitance Model* can be used to build a model that includes the phenomena of this problem and to perform the numerical integration.

### EXAMPLE 5.3

A 3-mm-thick panel of aluminum alloy ( $k = 177 \text{ W/m} \cdot \text{K}$ ,  $c = 875 \text{ J/kg} \cdot \text{K}$ , and  $\rho = 2770 \text{ kg/m}^3$ ) is finished on both sides with an epoxy coating that must be cured at or above  $T_c = 150^\circ\text{C}$  for at least 5 min. The production line for the curing operation involves two steps: (1) heating in a large oven with air at  $T_{\infty,o} = 175^\circ\text{C}$  and a convection coefficient of  $h_o = 40 \text{ W/m}^2 \cdot \text{K}$ , and (2) cooling in a large chamber with air at  $T_{\infty,c} = 25^\circ\text{C}$  and a convection coefficient of  $h_c = 10 \text{ W/m}^2 \cdot \text{K}$ . The heating portion of the process is conducted over a time interval  $t_e$ , which exceeds the time  $t_c$  required to reach  $150^\circ\text{C}$  by 5 min ( $t_e = t_c + 300 \text{ s}$ ). The coating has an emissivity of  $\epsilon = 0.8$ , and the temperatures of the oven and chamber walls are  $175^\circ\text{C}$  and  $25^\circ\text{C}$ , respectively. If the panel is placed in the oven at an initial temperature of  $25^\circ\text{C}$  and

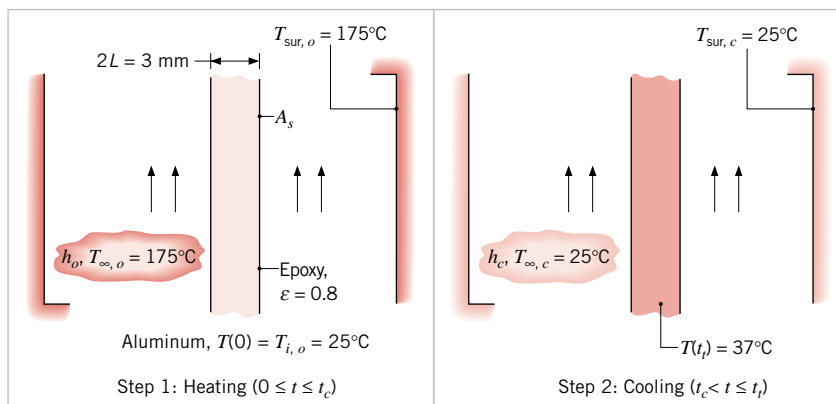
removed from the chamber at a *safe-to-touch* temperature of  $37^\circ\text{C}$ , what is the total elapsed time for the two-step curing operation?

### SOLUTION

**Known:** Operating conditions for a two-step heating/cooling process in which a coated aluminum panel is maintained at or above a temperature of  $150^\circ\text{C}$  for at least 5 min.

**Find:** Total time  $t_i$  required for the two-step process.

**Schematic:**



**Assumptions:**

1. Panel temperature is uniform at any instant.
2. Thermal resistance of epoxy is negligible.
3. Constant properties.

**Analysis:** To assess the validity of the lumped capacitance approximation, we begin by calculating Biot numbers for the heating and cooling processes.

$$Bi_h = \frac{h_o L}{k} = \frac{(40 \text{ W/m}^2 \cdot \text{K})(0.0015 \text{ m})}{177 \text{ W/m} \cdot \text{K}} = 3.4 \times 10^{-4}$$

$$Bi_c = \frac{h_c L}{k} = \frac{(10 \text{ W/m}^2 \cdot \text{K})(0.0015 \text{ m})}{177 \text{ W/m} \cdot \text{K}} = 8.5 \times 10^{-5}$$

Hence the lumped capacitance approximation is excellent.

To determine whether radiation exchange between the panel and its surroundings should be considered, the radiation heat transfer coefficient is determined from Equation 1.9. A representative value of  $h_r$  for the heating process is associated with the cure condition, in which case

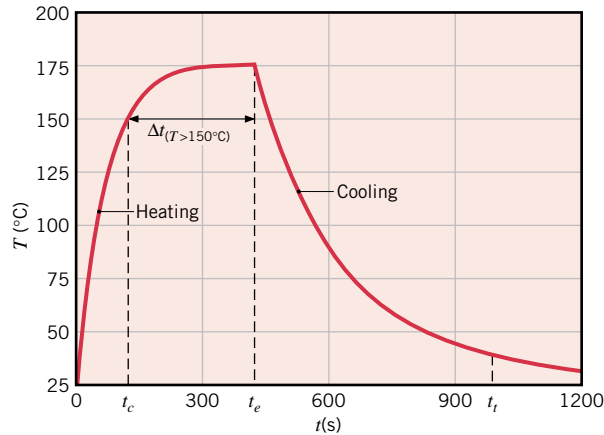
$$\begin{aligned} h_{r,o} &= \varepsilon \sigma (T_c + T_{\text{sur},o})(T_c^2 + T_{\text{sur},o}^2) \\ &= 0.8 \times 5.67 \times 10^{-8} \text{ W/m}^2 \cdot \text{K}^4 (423 + 448) \text{ K} (423^2 + 448^2) \text{ K}^2 \\ &= 15 \text{ W/m}^2 \cdot \text{K} \end{aligned}$$

Using  $T_c = 150^\circ\text{C}$  with  $T_{\text{sur},c} = 25^\circ\text{C}$  for the cooling process, we also obtain  $h_{r,c} = 8.8 \text{ W/m}^2 \cdot \text{K}$ . Since the values of  $h_{r,o}$  and  $h_{r,c}$  are comparable to those of  $h_o$  and  $h_c$ , respectively, radiation effects must be considered.

With  $V = 2LA_s$  and  $A_{s,c} = A_{s,r} = 2A_s$ , Equation 5.15 may be expressed as

$$\int_{T_i}^T dT = T(t) - T_i = -\frac{1}{\rho c L} \int_0^t [h(T - T_\infty) + \varepsilon \sigma (T^4 - T_{\text{sur}}^4)] dt$$

Selecting a suitable time increment  $\Delta t$ , the right-hand side of this equation may be evaluated numerically to obtain the panel temperature at  $t = \Delta t, 2\Delta t, 3\Delta t$ , and so on. At each new step of the calculation, the value of  $T$  computed from the previous time step is used in the integrand. Selecting  $\Delta t = 10 \text{ s}$ , calculations for the heating process are extended to  $t_e = t_c + 300 \text{ s}$ , which is 5 min beyond the time required for the panel to reach  $T_c = 150^\circ\text{C}$ . At  $t_e$  the cooling process is initiated and continued until the panel temperature reaches  $37^\circ\text{C}$  at  $t = t_t$ . The integration was performed using a fourth-order Runge-Kutta scheme, and results of the calculations are plotted as follows:



The total time for the two-step process is

$$t_t = 989 \text{ s}$$

with intermediate times of  $t_c = 124 \text{ s}$  and  $t_e = 424 \text{ s}$ .

### Comments:

1. Generally, the accuracy of a numerical integration improves with decreasing  $\Delta t$ , but at the expense of increased computation time. In this case, however, results obtained for  $\Delta t = 1 \text{ s}$  are virtually identical to those obtained for  $\Delta t = 10 \text{ s}$ , indicating that the larger time interval is sufficient to accurately depict the temperature history.
2. The duration of the two-step process may be reduced by increasing the convection coefficients and/or by reducing the period of extended heating. The second option is made possible by the fact that, during a portion of the cooling period, the panel temperature remains above  $150^\circ\text{C}$ . Hence, to satisfy the cure requirement, it is not necessary to extend heating for as much as 5 min from  $t = t_c$ . If the convection coefficients are increased to  $h_o = h_c = 100 \text{ W/m}^2 \cdot \text{K}$  and an

extended heating period of 300 s is maintained, the numerical integration yields  $t_c = 58$  s and  $t_f = 445$  s. The corresponding time interval over which the panel temperature exceeds  $150^\circ\text{C}$  is  $\Delta t_{(T>150^\circ\text{C})} = 306$  s ( $58 \text{ s} \leq t \leq 364 \text{ s}$ ). If the extended heating period is reduced to 294 s, the numerical integration yields  $t_c = 58$  s,  $t_f = 439$  s, and  $\Delta t_{(T>150^\circ\text{C})} = 300$  s. Hence the total process time is reduced, while the curing requirement is still satisfied.

3. The solution for this example is provided as a ready-to-solve model in *IHT*, with annotations on how the code is written and solved. Look under *Examples* on the *Toolbar*. Note how the *User-Defined Function* feature of *IHT* (\*.udf) is used to represent the time dependence of the ambient temperature in the two-step heating and cooling process, thereby allowing use of a single form of the energy balance relation for the entire process. The model can be used to check the results of Comment 2 or to independently explore modifications of the cure process.

## 5.4

### Spatial Effects

Situations frequently arise for which the lumped capacitance method is inappropriate, and alternative approaches must be used. Regardless of the particular method, we must now cope with the fact that temperature gradients within the medium are no longer negligible.

In their most general form, transient conduction problems are described by the heat equation, Equation 2.17, for rectangular coordinates or Equations 2.24 and 2.27, respectively, for cylindrical and spherical coordinates. The solutions to these partial differential equations provide the variation of temperature with both time and the spatial coordinates. However, in many problems, such as the plane wall of Figure 5.4, only one spatial coordinate is needed to describe the internal temperature distribution. With no internal generation and the assumption of constant thermal conductivity, Equation 2.17 then reduces to

$$\frac{\partial^2 T}{\partial x^2} = \frac{1}{\alpha} \frac{\partial T}{\partial t} \quad (5.26)$$

To solve Equation 5.26 for the temperature distribution  $T(x, t)$ , it is necessary to specify an *initial* condition and two *boundary conditions*. For the typical transient conduction problem of Figure 5.4, the initial condition is

$$T(x, 0) = T_i \quad (5.27)$$

and the boundary conditions are

$$\left. \frac{\partial T}{\partial x} \right|_{x=0} = 0 \quad (5.28)$$



and

$$-k \frac{\partial T}{\partial x} \Big|_{x=L} = h[T(L, t) - T_\infty] \quad (5.29)$$

Equation 5.27 presumes a uniform temperature distribution at time  $t = 0$ ; Equation 5.28 reflects the *symmetry requirement* for the midplane of the wall; and Equation 5.29 describes the surface condition experienced for time  $t > 0$ . From Equations 5.26 through 5.29, it is evident that, in addition to depending on  $x$  and  $t$ , temperatures in the wall also depend on a number of physical parameters. In particular

$$T = T(x, t, T_i, T_\infty, L, k, \alpha, h) \quad (5.30)$$

The foregoing problem may be solved analytically or numerically. These methods will be considered in subsequent sections, but first it is important to note the advantages that may be obtained by *nondimensionalizing* the governing equations. This may be done by arranging the relevant variables into suitable *groups*. Consider the dependent variable  $T$ . If the temperature difference  $\theta \equiv T - T_\infty$  is divided by the *maximum possible temperature difference*  $\theta_i \equiv T_i - T_\infty$ , a dimensionless form of the dependent variable may be defined as

$$\theta^* \equiv \frac{\theta}{\theta_i} = \frac{T - T_\infty}{T_i - T_\infty} \quad (5.31)$$

Accordingly,  $\theta^*$  must lie in the range  $0 \leq \theta^* \leq 1$ . A dimensionless spatial coordinate may be defined as

$$x^* \equiv \frac{x}{L} \quad (5.32)$$

where  $L$  is the half-thickness of the plane wall, and a dimensionless time may be defined as

$$t^* \equiv \frac{\alpha t}{L^2} \equiv Fo \quad (5.33)$$

where  $t^*$  is equivalent to the dimensionless *Fourier number*, Equation 5.12.

Substituting the definitions of Equations 5.31 through 5.33 into Equations 5.26 through 5.29, the heat equation becomes

$$\frac{\partial^2 \theta^*}{\partial x^{*2}} = \frac{\partial \theta^*}{\partial Fo} \quad (5.34)$$

and the initial and boundary conditions become

$$\theta^*(x^*, 0) = 1 \quad (5.35)$$

$$\frac{\partial \theta^*}{\partial x^*} \Big|_{x^*=0} = 0 \quad (5.36)$$

and

$$\frac{\partial \theta^*}{\partial x^*} \Big|_{x^*=1} = -Bi \theta^*(1, t^*) \quad (5.37)$$

where the *Biot number* is  $Bi \equiv hL/k$ . In dimensionless form the functional dependence may now be expressed as

$$\theta^* = f(x^*, Fo, Bi) \quad (5.38)$$

Recall that a similar functional dependence, without the  $x^*$  variation, was obtained for the lumped capacitance method, as shown in Equation 5.13.

Although the Fourier number may be viewed as a dimensionless time, it has an important physical interpretation when used in problems for which heat transfer by conduction through a solid is concurrent with thermal energy storage by the solid. With a characteristic length of  $L$ , the temperature gradient across a solid and the cross-sectional area perpendicular to conduction heat transfer may be approximated as  $\Delta T/L$  and  $L^2$ , respectively. Hence, as a first-order approximation, the heat rate may be expressed as  $q \sim kL^2\Delta T/L$ . Similarly, with the volume of the solid represented as  $V \sim L^3$ , the rate of change of thermal energy storage by the solid may be approximated as  $\dot{E}_{st} \sim \rho L^3 c \Delta T/t$ . It follows that  $(q/\dot{E}_{st}) \sim kt/\rho c L^2 = \alpha t/L^2 = Fo$ . Hence, the Fourier number provides a measure of the relative effectiveness with which a solid conducts and stores thermal energy.

Comparing Equations 5.30 and 5.38, the considerable advantage associated with casting the problem in dimensionless form becomes apparent. Equation 5.38 implies that *for a prescribed geometry, the transient temperature distribution is a universal function of  $x^*$ ,  $Fo$ , and  $Bi$* . That is, the *dimensionless solution* has a prescribed form that does not depend on the particular value of  $T_i$ ,  $T_\infty$ ,  $L$ ,  $k$ ,  $\alpha$ , or  $h$ . Since this generalization greatly simplifies the presentation and utilization of transient solutions, the dimensionless variables are used extensively in subsequent sections.

## 5.5

### The Plane Wall with Convection

Exact, analytical solutions to transient conduction problems have been obtained for many simplified geometries and boundary conditions and are well documented [1–4]. Several mathematical techniques, including the method of separation of variables (Section 4.2), may be used for this purpose, and typically the solution for the dimensionless temperature distribution, Equation 5.38, is in the form of an infinite series. However, except for very small values of the Fourier number, this series may be approximated by a single term.

#### 5.5.1 Exact Solution

Consider the *plane wall* of thickness  $2L$  (Figure 5.6a). If the thickness is small relative to the width and height of the wall, it is reasonable to assume that conduction occurs exclusively in the  $x$  direction. If the wall is initially at a uniform temperature,  $T(x, 0) = T_i$ , and is suddenly immersed in a fluid of  $T_\infty \neq T_i$ , the resulting temperatures may be obtained by solving Equation 5.34 subject to the conditions of Equations 5.35 through 5.37. Since the convection conditions for the surfaces at

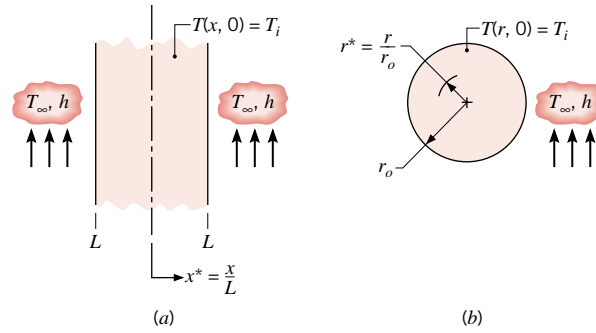


**FIGURE 5.6** One-dimensional systems with an initial uniform temperature subjected to sudden convection conditions. (a) Plane wall. (b) Infinite cylinder or sphere.

$x^* = \pm 1$  are the same, the temperature distribution at any instant must be symmetrical about the midplane ( $x^* = 0$ ). An exact solution to this problem is of the form [2]

$$\theta^* = \sum_{n=1}^{\infty} C_n \exp(-\zeta_n^2 Fo) \cos(\zeta_n x^*) \quad (5.39a)$$

where  $Fo = \alpha t/L^2$ , the coefficient  $C_n$  is

$$C_n = \frac{4 \sin \zeta_n}{2\zeta_n + \sin(2\zeta_n)} \quad (5.39b)$$

and the discrete values of  $\zeta_n$  (*eigenvalues*) are positive roots of the transcendental equation

$$\zeta_n \tan \zeta_n = Bi \quad (5.39c)$$

The first four roots of this equation are given in Appendix B.3.

### 5.5.2 Approximate Solution

It can be shown (Problem 5.34) that for values of  $Fo > 0.2$ , the infinite series solution, Equation 5.39a, can be approximated by the first term of the series. Invoking this approximation, the dimensionless form of the temperature distribution becomes

$$\theta^* = C_1 \exp(-\zeta_1^2 Fo) \cos(\zeta_1 x^*) \quad (5.40a)$$


or

$$\theta^* = \theta_o^* \cos(\zeta_1 x^*) \quad (5.40b)$$

where  $\theta_o^* \equiv (T_o - T_\infty)/(T_i - T_\infty)$  represents the midplane ( $x^* = 0$ ) temperature

$$\theta_o^* = C_1 \exp(-\zeta_1^2 Fo) \quad (5.41)$$

An important implication of Equation 5.40b is that *the time dependence of the temperature at any location within the wall is the same as that of the midplane temperature*. The coefficients  $C_1$  and  $\zeta_1$  are evaluated from Equations 5.39b and 5.39c, respectively, and are given in Table 5.1 for a range of Biot numbers.

 Graphical representations of the one-term approximations are presented in Section 5S.1.

**TABLE 5.1** Coefficients used in the one-term approximation to the series solutions for transient one-dimensional conduction

$Bi^a$	Plane Wall		Infinite Cylinder		Sphere	
	$\zeta_1$ (rad)	$C_1$	$\zeta_1$ (rad)	$C_1$	$\zeta_1$ (rad)	$C_1$
0.01	0.0998	1.0017	0.1412	1.0025	0.1730	1.0030
0.02	0.1410	1.0033	0.1995	1.0050	0.2445	1.0060
0.03	0.1723	1.0049	0.2440	1.0075	0.2991	1.0090
0.04	0.1987	1.0066	0.2814	1.0099	0.3450	1.0120
0.05	0.2218	1.0082	0.3143	1.0124	0.3854	1.0149
0.06	0.2425	1.0098	0.3438	1.0148	0.4217	1.0179
0.07	0.2615	1.0114	0.3709	1.0173	0.4551	1.0209
0.08	0.2791	1.0130	0.3960	1.0197	0.4860	1.0239
0.09	0.2956	1.0145	0.4195	1.0222	0.5150	1.0268
0.10	0.3111	1.0161	0.4417	1.0246	0.5423	1.0298
0.15	0.3779	1.0237	0.5376	1.0365	0.6609	1.0445
0.20	0.4328	1.0311	0.6170	1.0483	0.7593	1.0592
0.25	0.4801	1.0382	0.6856	1.0598	0.8447	1.0737
0.30	0.5218	1.0450	0.7465	1.0712	0.9208	1.0880
0.4	0.5932	1.0580	0.8516	1.0932	1.0528	1.1164
0.5	0.6533	1.0701	0.9408	1.1143	1.1656	1.1441
0.6	0.7051	1.0814	1.0184	1.1345	1.2644	1.1713
0.7	0.7506	1.0919	1.0873	1.1539	1.3525	1.1978
0.8	0.7910	1.1016	1.1490	1.1724	1.4320	1.2236
0.9	0.8274	1.1107	1.2048	1.1902	1.5044	1.2488
1.0	0.8603	1.1191	1.2558	1.2071	1.5708	1.2732
2.0	1.0769	1.1785	1.5994	1.3384	2.0288	1.4793
3.0	1.1925	1.2102	1.7887	1.4191	2.2889	1.6227
4.0	1.2646	1.2287	1.9081	1.4698	2.4556	1.7202
5.0	1.3138	1.2402	1.9898	1.5029	2.5704	1.7870
6.0	1.3496	1.2479	2.0490	1.5253	2.6537	1.8338
7.0	1.3766	1.2532	2.0937	1.5411	2.7165	1.8673
8.0	1.3978	1.2570	2.1286	1.5526	1.7654	1.8920
9.0	1.4149	1.2598	2.1566	1.5611	2.8044	1.9106
10.0	1.4289	1.2620	2.1795	1.5677	2.8363	1.9249
20.0	1.4961	1.2699	2.2881	1.5919	2.9857	1.9781
30.0	1.5202	1.2717	2.3261	1.5973	3.0372	1.9898
40.0	1.5325	1.2723	2.3455	1.5993	3.0632	1.9942
50.0	1.5400	1.2727	2.3572	1.6002	3.0788	1.9962
100.0	1.5552	1.2731	2.3809	1.6015	3.1102	1.9990
$\infty$	1.5708	1.2733	2.4050	1.6018	3.1415	2.0000

<sup>a</sup> $Bi = hL/k$  for the plane wall and  $hr_o/k$  for the infinite cylinder and sphere. See Figure 5.6.

### 5.5.3 Total Energy Transfer

In many situations it is useful to know the total energy that has left (or entered) the wall up to any time  $t$  in the transient process. The conservation of energy requirement,

Equation 1.11b, may be applied for the time interval bounded by the initial condition ( $t = 0$ ) and any time  $t > 0$

$$E_{\text{in}} - E_{\text{out}} = \Delta E_{\text{st}} \quad (5.42)$$

Equating the energy transferred from the wall  $Q$  to  $E_{\text{out}}$  and setting  $E_{\text{in}} = 0$  and  $\Delta E_{\text{st}} = E(t) - E(0)$ , it follows that

$$Q = -[E(t) - E(0)] \quad (5.43a)$$

or

$$Q = - \int \rho c [T(x, t) - T_i] dV \quad (5.43b)$$

where the integration is performed over the volume of the wall. It is convenient to nondimensionalize this result by introducing the quantity

$$Q_o = \rho c V (T_i - T_\infty) \quad (5.44)$$

which may be interpreted as the initial internal energy of the wall relative to the fluid temperature. It is also the *maximum* amount of energy transfer that could occur if the process were continued to time  $t = \infty$ . Hence, assuming constant properties, the ratio of the total energy transferred from the wall over the time interval  $t$  to the maximum possible transfer is

$$\frac{Q}{Q_o} = \int \frac{-[T(x, t) - T_i]}{T_i - T_\infty} \frac{dV}{V} = \frac{1}{V} \int (1 - \theta^*) dV \quad (5.45)$$

Employing the approximate form of the temperature distribution for the plane wall, Equation 5.40b, the integration prescribed by Equation 5.45 can be performed to obtain

$$\frac{Q}{Q_o} = 1 - \frac{\sin \zeta_1}{\zeta_1} \theta_o^* \quad (5.46)$$

where  $\theta_o^*$  can be determined from Equation 5.41, using Table 5.1 for values of the coefficients  $C_1$  and  $\zeta_1$ .

### 5.5.4 Additional Considerations

Because the mathematical problem is precisely the same, the foregoing results may also be applied to a plane wall of thickness  $L$ , which is insulated on one side ( $x^* = 0$ ) and experiences convective transport on the other side ( $x^* = +1$ ). This equivalence is a consequence of the fact that, regardless of whether a symmetrical or an adiabatic requirement is prescribed at  $x^* = 0$ , the boundary condition is of the form  $\partial \theta^* / \partial x^* = 0$ .

It should also be noted that the foregoing results may be used to determine the transient response of a plane wall to a sudden change in *surface* temperature. The process is equivalent to having an infinite convection coefficient, in which case the Biot number is infinite ( $Bi = \infty$ ) and the fluid temperature  $T_\infty$  is replaced by the prescribed surface temperature  $T_s$ .

## 5.6

### Radial Systems with Convection

For an infinite cylinder or sphere of radius  $r_o$  (Figure 5.6b), which is at an initial uniform temperature and experiences a change in convective conditions, results similar to those of Section 5.5 may be developed. That is, an exact series solution may be obtained for the time dependence of the radial temperature distribution, and a one-term approximation may be used for most conditions. The infinite cylinder is an idealization that permits the assumption of one-dimensional conduction in the radial direction. It is a reasonable approximation for cylinders having  $L/r_o \geq 10$ .

#### 5.6.1 Exact Solutions

For a uniform initial temperature and convective boundary conditions, the exact solutions [2] are as follows.

**Infinite Cylinder** In dimensionless form, the temperature is

$$\theta^* = \sum_{n=1}^{\infty} C_n \exp(-\zeta_n^2 Fo) J_0(\zeta_n r^*) \quad (5.47a)$$

where  $Fo = \alpha t/r_o^2$ ,

$$C_n = \frac{2}{\zeta_n} \frac{J_1(\zeta_n)}{J_0^2(\zeta_n) + J_1^2(\zeta_n)} \quad (5.47b)$$

and the discrete values of  $\zeta_n$  are positive roots of the transcendental equation

$$\zeta_n \frac{J_1(\zeta_n)}{J_0(\zeta_n)} = Bi \quad (5.47c)$$

where  $Bi = hr_o/k$ . The quantities  $J_1$  and  $J_0$  are Bessel functions of the first kind and their values are tabulated in Appendix B.4. Roots of the transcendental equation (5.47c) are tabulated by Schneider [2].

**Sphere** Similarly, for the sphere

$$\theta^* = \sum_{n=1}^{\infty} C_n \exp(-\zeta_n^2 Fo) \frac{1}{\zeta_n r^*} \sin(\zeta_n r^*) \quad (5.48a)$$

where  $Fo = \alpha t/r_o^2$ ,

$$C_n = \frac{4[\sin(\zeta_n) - \zeta_n \cos(\zeta_n)]}{2\zeta_n - \sin(2\zeta_n)} \quad (5.48b)$$

and the discrete values of  $\zeta_n$  are positive roots of the transcendental equation

$$1 - \zeta_n \cot \zeta_n = Bi \quad (5.48c)$$

where  $Bi = hr_o/k$ . Roots of the transcendental equation are tabulated by Schneider [2].

### 5.6.2 Approximate Solutions

For the infinite cylinder and sphere, the foregoing series solutions can again be approximated by a single term for  $Fo > 0.2$ . Hence, as for the case of the plane wall, the time dependence of the temperature at any location within the radial system is the same as that of the centerline or centerpoint.

**Infinite Cylinder** The one-term approximation to Equation 5.47a is

$$\theta^* = C_1 \exp(-\zeta_1^2 Fo) J_0(\zeta_1 r^*) \quad (5.49a)$$

or

$$\theta^* = \theta_o^* J_0(\zeta_1 r^*) \quad (5.49b)$$

where  $\theta_o^*$  represents the centerline temperature and is of the form

$$\theta_o^* = C_1 \exp(-\zeta_1^2 Fo) \quad (5.49c)$$

Values of the coefficients  $C_1$  and  $\zeta_1$  have been determined and are listed in Table 5.1 for a range of Biot numbers.

**Sphere** From Equation 5.48a, the one-term approximation is

$$\theta^* = C_1 \exp(-\zeta_1^2 Fo) \frac{1}{\zeta_1 r^*} \sin(\zeta_1 r^*) \quad (5.50a)$$

or

$$\theta^* = \theta_o^* \frac{1}{\zeta_1 r^*} \sin(\zeta_1 r^*) \quad (5.50b)$$

where  $\theta_o^*$  represents the center temperature and is of the form

$$\theta_o^* = C_1 \exp(-\zeta_1^2 Fo) \quad (5.50c)$$

Values of the coefficients  $C_1$  and  $\zeta_1$  have been determined and are listed in Table 5.1 for a range of Biot numbers.

### 5.6.3 Total Energy Transfer


As in Section 5.5.3, an energy balance may be performed to determine the total energy transfer from the infinite cylinder or sphere over the time interval  $\Delta t = t$ . Substituting from the approximate solutions, Equations 5.49b and 5.50b, and introducing  $Q_o$  from Equation 5.44, the results are as follows.


**Infinite Cylinder**

$$\frac{Q}{Q_o} = 1 - \frac{2\theta_o^*}{\zeta_1} J_1(\zeta_1) \quad (5.51)$$

**Sphere**

$$\frac{Q}{Q_o} = 1 - \frac{3\theta_o^*}{\zeta_1^3} [\sin(\zeta_1) - \zeta_1 \cos(\zeta_1)] \quad (5.52)$$

 Graphical representations of the one-term approximations are presented in Section 5S.1.

 Graphical representations of the one-term approximations are presented in Section 5S.1.

Values of the center temperature  $\theta_o^*$  are determined from Equation 5.49c or 5.50c, using the coefficients of Table 5.1 for the appropriate system.

### 5.6.4 Additional Considerations

As for the plane wall, the foregoing results may be used to predict the transient response of long cylinders and spheres subjected to a sudden change in *surface* temperature. Namely, an infinite Biot number is prescribed, and the fluid temperature  $T_\infty$  is replaced by the constant surface temperature  $T_s$ .

#### EXAMPLE 5.4

Consider a steel pipeline (AISI 1010) that is 1 m in diameter and has a wall thickness of 40 mm. The pipe is heavily insulated on the outside, and before the initiation of flow, the walls of the pipe are at a uniform temperature of  $-20^\circ\text{C}$ . With the initiation of flow, hot oil at  $60^\circ\text{C}$  is pumped through the pipe, creating a convective condition corresponding to  $h = 500 \text{ W/m}^2 \cdot \text{K}$  at the inner surface of the pipe.

1. What are the appropriate Biot and Fourier numbers 8 min after the initiation of flow?
2. At  $t = 8 \text{ min}$ , what is the temperature of the exterior pipe surface covered by the insulation?
3. What is the heat flux  $q''$  ( $\text{W/m}^2$ ) to the pipe from the oil at  $t = 8 \text{ min}$ ?
4. How much energy per meter of pipe length has been transferred from the oil to the pipe at  $t = 8 \text{ min}$ ?

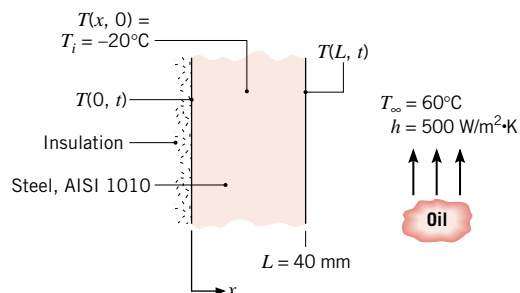
#### SOLUTION

**Known:** Wall subjected to sudden change in convective surface condition.

#### Find:

1. Biot and Fourier numbers after 8 min.
2. Temperature of exterior pipe surface after 8 min.
3. Heat flux to the wall at 8 min.
4. Energy transferred to pipe per unit length after 8 min.

#### Schematic:





**Assumptions:**

1. Pipe wall can be approximated as plane wall, since thickness is much less than diameter.
2. Constant properties.
3. Outer surface of pipe is adiabatic.

**Properties:** Table A.1, steel type AISI 1010 [ $T = (-20 + 60)^\circ\text{C}/2 \approx 300\text{ K}$ ]:  
 $\rho = 7832\text{ kg/m}^3$ ,  $c = 434\text{ J/kg} \cdot \text{K}$ ,  $k = 63.9\text{ W/m} \cdot \text{K}$ ,  $\alpha = 18.8 \times 10^{-6}\text{ m}^2/\text{s}$ .

**Analysis:**

1. At  $t = 8\text{ min}$ , the Biot and Fourier numbers are computed from Equations 5.10 and 5.12, respectively, with  $L_c = L$ . Hence

$$Bi = \frac{hL}{k} = \frac{500\text{ W/m}^2 \cdot \text{K} \times 0.04\text{ m}}{63.9\text{ W/m} \cdot \text{K}} = 0.313 \quad \triangleleft$$

$$Fo = \frac{\alpha t}{L^2} = \frac{18.8 \times 10^{-6}\text{ m}^2/\text{s} \times 8\text{ min} \times 60\text{ s/min}}{(0.04\text{ m})^2} = 5.64 \quad \triangleleft$$

2. With  $Bi = 0.313$ , use of the lumped capacitance method is inappropriate. However, since  $Fo > 0.2$  and transient conditions in the insulated pipe wall of thickness  $L$  correspond to those in a plane wall of thickness  $2L$  experiencing the same surface condition, the desired results may be obtained from the one-term approximation for a plane wall. The midplane temperature can be determined from Equation 5.41

$$\theta_o^* = \frac{T_o - T_\infty}{T_i - T_\infty} = C_1 \exp(-\zeta_1^2 Fo)$$

where, with  $Bi = 0.313$ ,  $C_1 = 1.047$  and  $\zeta_1 = 0.531\text{ rad}$  from Table 5.1. With  $Fo = 5.64$ ,

$$\theta_o^* = 1.047 \exp[-(0.531\text{ rad})^2 \times 5.64] = 0.214$$

Hence after 8 min, the temperature of the exterior pipe surface, which corresponds to the midplane temperature of a plane wall, is

$$T(0, 8\text{ min}) = T_\infty + \theta_o^*(T_i - T_\infty) = 60^\circ\text{C} + 0.214(-20 - 60)^\circ\text{C} = 42.9^\circ\text{C} \quad \triangleleft$$

3. Heat transfer to the inner surface at  $x = L$  is by convection, and at any time  $t$  the heat flux may be obtained from Newton's law of cooling. Hence at  $t = 480\text{ s}$ ,

$$q_x''(L, 480\text{ s}) \equiv q_L'' = h[T(L, 480\text{ s}) - T_\infty]$$

Using the one-term approximation for the surface temperature, Equation 5.40b with  $x^* = 1$  has the form

$$\theta^* = \theta_o^* \cos(\zeta_1)$$

$$T(L, t) = T_\infty + (T_i - T_\infty)\theta_o^* \cos(\zeta_1)$$

$$T(L, 8\text{ min}) = 60^\circ\text{C} + (-20 - 60)^\circ\text{C} \times 0.214 \times \cos(0.531\text{ rad})$$

$$T(L, 8\text{ min}) = 45.2^\circ\text{C}$$

The heat flux at  $t = 8$  min is then

$$q_L'' = 500 \text{ W/m}^2 \cdot \text{K} (45.2 - 60)^\circ\text{C} = -7400 \text{ W/m}^2 \quad \triangleleft$$

4. The energy transfer to the pipe wall over the 8-min interval may be obtained from Equations 5.44 and 5.46. With

$$\frac{Q}{Q_o} = 1 - \frac{\sin(\xi_1)}{\xi_1} \theta_o^*$$

$$\frac{Q}{Q_o} = 1 - \frac{\sin(0.531 \text{ rad})}{0.531 \text{ rad}} \times 0.214 = 0.80$$

it follows that

$$Q = 0.80 \rho c V (T_i - T_\infty)$$

or with a volume per unit pipe length of  $V' = \pi DL$ ,

$$Q' = 0.80 \rho c \pi DL (T_i - T_\infty)$$

$$Q' = 0.80 \times 7832 \text{ kg/m}^3 \times 434 \text{ J/kg} \cdot \text{K}$$

$$\times \pi \times 1 \text{ m} \times 0.04 \text{ m} (-20 - 60)^\circ\text{C}$$

$$Q' = -2.73 \times 10^7 \text{ J/m} \quad \triangleleft$$

### Comments:

1. The minus sign associated with  $q''$  and  $Q'$  simply implies that the direction of heat transfer is from the oil to the pipe (into the pipe wall).
2. The foregoing results may be obtained using the *IHT Models, Transient Conduction, Plane Wall* option. The model provides for calculation of the temperature distribution,  $T(x, t)$ , the heat flux distribution,  $q_x''(x, t)$ , and the amount of energy transferred from the wall,  $Q(t)$ . Substituting the appropriate input parameters for the wall geometry, thermophysical properties and thermal conditions, the model yields the following results:

$$\begin{aligned} T(0, 8 \text{ min}) &= 43.1^\circ\text{C} & q_L''(L, 8 \text{ min}) &= q_L'' = -7305 \text{ W/m}^2 \\ T(L, 8 \text{ min}) &= 45.4^\circ\text{C} & Q'(8 \text{ min}) &= -2.724 \times 10^7 \text{ J/m} \end{aligned}$$

Since the *IHT* model uses a multiple-term approximation to the series solution, the results are more accurate than those obtained from the foregoing one-term approximation. The complete solution for this example is provided as a ready-to-solve model in *IHT*, with annotations on how the code is written and solved (see *Examples*). *IHT Models for Transient Conduction* are also provided for the radial systems treated in Section 5.6.

### EXAMPLE 5.5

A new process for treatment of a special material is to be evaluated. The material, a sphere of radius  $r_o = 5$  mm, is initially in equilibrium at  $400^\circ\text{C}$  in a furnace. It is suddenly removed from the furnace and subjected to a two-step cooling process.

**Step 1** Cooling in air at  $20^\circ\text{C}$  for a period of time  $t_a$  until the center temperature reaches a critical value,  $T_a(0, t_a) = 335^\circ\text{C}$ . For this situation, the convective heat transfer coefficient is  $h_a = 10 \text{ W/m}^2 \cdot \text{K}$ .

After the sphere has reached this critical temperature, the second step is initiated.

**Step 2** Cooling in a well-stirred water bath at  $20^\circ\text{C}$ , with a convective heat transfer coefficient of  $h_w = 6000 \text{ W/m}^2 \cdot \text{K}$ .

The thermophysical properties of the material are  $\rho = 3000 \text{ kg/m}^3$ ,  $k = 20 \text{ W/m} \cdot \text{K}$ ,  $c = 1000 \text{ J/kg} \cdot \text{K}$ , and  $\alpha = 6.66 \times 10^{-6} \text{ m}^2/\text{s}$ .

1. Calculate the time  $t_a$  required for step 1 of the cooling process to be completed.
2. Calculate the time  $t_w$  required during step 2 of the process for the center of the sphere to cool from  $335^\circ\text{C}$  (the condition at the completion of step 1) to  $50^\circ\text{C}$ .

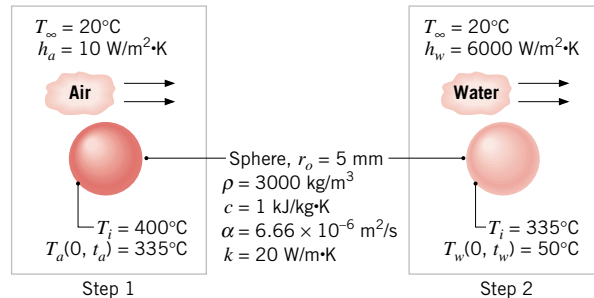
### SOLUTION

**Known:** Temperature requirements for cooling a sphere.

**Find:**

1. Time  $t_a$  required to accomplish desired cooling in air.
2. Time  $t_w$  required to complete cooling in water bath.

**Schematic:**



**Assumptions:**

1. One-dimensional conduction in  $r$ .
2. Constant properties.

**Analysis:**

1. To determine whether the lumped capacitance method can be used, the Biot number is calculated. From Equation 5.10, with  $L_c = r_o/3$ ,

$$Bi = \frac{h_a r_o}{3k} = \frac{10 \text{ W/m}^2 \cdot \text{K} \times 0.005 \text{ m}}{3 \times 20 \text{ W/m} \cdot \text{K}} = 8.33 \times 10^{-4}$$

Accordingly, the lumped capacitance method may be used, and the temperature is nearly uniform throughout the sphere. From Equation 5.5 it follows that

$$t_a = \frac{\rho V c}{h_a A_s} \ln \frac{\theta_i}{\theta_a} = \frac{\rho r_o c}{3 h_a} \ln \frac{T_i - T_\infty}{T_a - T_\infty}$$

where  $V = (4/3)\pi r_o^3$  and  $A_s = 4\pi r_o^2$ . Hence

$$t_a = \frac{3000 \text{ kg/m}^3 \times 0.005 \text{ m} \times 1000 \text{ J/kg} \cdot \text{K}}{3 \times 10 \text{ W/m}^2 \cdot \text{K}} \ln \frac{400 - 20}{335 - 20} = 94 \text{ s} \quad \triangleleft$$

2. To determine whether the lumped capacitance method may also be used for the second step of the cooling process, the Biot number is again calculated. In this case

$$Bi = \frac{h_w r_o}{3k} = \frac{6000 \text{ W/m}^2 \cdot \text{K} \times 0.005 \text{ m}}{3 \times 20 \text{ W/m} \cdot \text{K}} = 0.50$$

and the lumped capacitance method is not appropriate. However, to an excellent approximation, the temperature of the sphere is uniform at  $t = t_a$  and the one-term approximation may be used for the calculations. The time  $t_w$  at which the center temperature reaches  $50^\circ\text{C}$ , that is,  $T(0, t_w) = 50^\circ\text{C}$ , can be obtained by rearranging Equation 5.50c

$$Fo = -\frac{1}{\zeta_1^2} \ln \left[ \frac{\theta_o^*}{C_1} \right] = -\frac{1}{\zeta_1^2} \ln \left[ \frac{1}{C_1} \times \frac{T(0, t_w) - T_\infty}{T_i - T_\infty} \right]$$

where  $t_w = Fo r_o^2 / \alpha$ . With the Biot number now defined as

$$Bi = \frac{h_w r_o}{k} = \frac{6000 \text{ W/m}^2 \cdot \text{K} \times 0.005 \text{ m}}{20 \text{ W/m} \cdot \text{K}} = 1.50$$

Table 5.1 yields  $C_1 = 1.376$  and  $\zeta_1 = 1.800$  rad. It follows that

$$Fo = -\frac{1}{(1.800 \text{ rad})^2} \ln \left[ \frac{1}{1.376} \times \frac{(50 - 20)^\circ\text{C}}{(335 - 20)^\circ\text{C}} \right] = 0.82$$

and

$$t_w = Fo \frac{r_o^2}{\alpha} = 0.82 \frac{(0.005 \text{ m})^2}{6.66 \times 10^{-6} \text{ m}^2/\text{s}} = 3.1 \text{ s} \quad \triangleleft$$

Note that, with  $Fo = 0.82$ , use of the one-term approximation is justified.

### Comments:

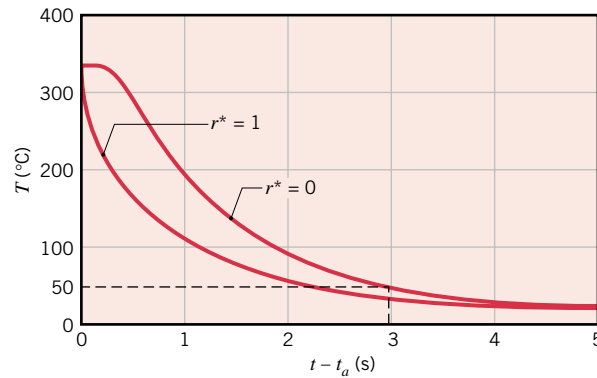
1. If the temperature distribution in the sphere at the conclusion of step 1 were not uniform, the one-term approximation could not be used for the calculations of step 2.
2. The surface temperature of the sphere at the conclusion of step 2 may be obtained from Equation 5.50b. With  $\theta_o^* = 0.095$  and  $r^* = 1$ ,

$$\theta^*(r_o) = \frac{T(r_o) - T_\infty}{T_i - T_\infty} = \frac{0.095}{1.800 \text{ rad}} \sin(1.800 \text{ rad}) = 0.0514$$

and

$$T(r_o) = 20^\circ\text{C} + 0.0514(335 - 20)^\circ\text{C} = 36^\circ\text{C}$$

The infinite series, Equation 5.48a, and its one-term approximation, Equation 5.50b, may be used to compute the temperature at any location in the sphere and at any time  $t > t_a$ . For  $(t - t_a) < 0.2(0.005 \text{ m})^2/6.66 \times 10^{-6} \text{ m}^2/\text{s} = 0.75 \text{ s}$ , a sufficient number of terms must be retained to ensure convergence of the series. For  $(t - t_a) > 0.75 \text{ s}$ , satisfactory convergence is provided by the one-term approximation. Computing and plotting the temperature histories for  $r = 0$  and  $r = r_o$ , we obtain the following results for  $0 \leq (t - t_a) \leq 5 \text{ s}$ :



3. The *IHT Models, Transient Conduction, Sphere* option could be used to analyze the cooling processes experienced by the sphere in air and water, steps 1 and 2. The *IHT Models, Lumped Capacitance* option may only be used to analyze the air-cooling process, step 1.

## 5.7

### The Semi-Infinite Solid

Another simple geometry for which analytical solutions may be obtained is the *semi-infinite solid*. Since, in principle, such a solid extends to infinity in all but one direction, it is characterized by a single identifiable surface (Figure 5.7). If a sudden change of conditions is imposed at this surface, transient, one-dimensional conduction will occur within the solid. The semi-infinite solid provides a *useful idealization* for many practical problems. It may be used to determine transient heat transfer near the surface of the earth or to approximate the transient response of a finite solid, such as a thick slab. For this second situation the approximation would be reasonable for the early portion of the transient, during which temperatures in the slab interior (well removed from the surface) are essentially uninfluenced by the change in surface conditions.

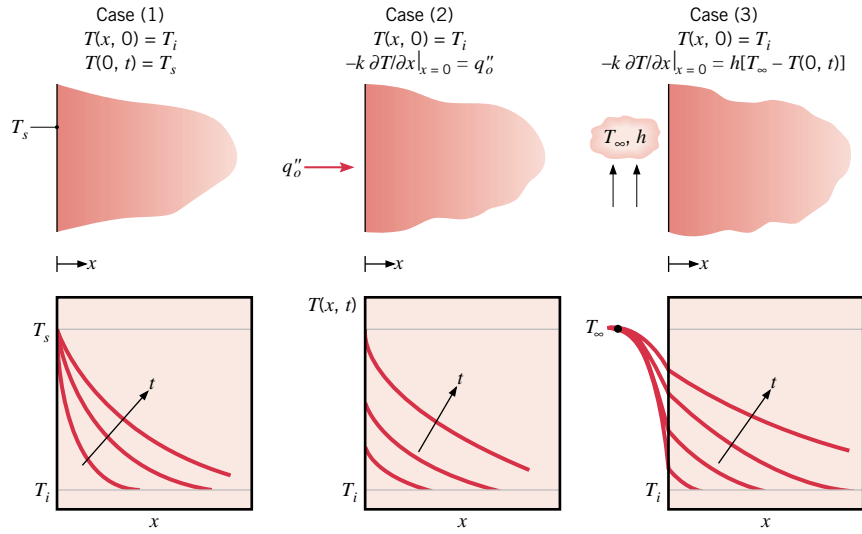


**FIGURE 5.7** Transient temperature distributions in a semi-infinite solid for three surface conditions: constant surface temperature, constant surface heat flux, and surface convection.

The heat equation for transient conduction in a semi-infinite solid is given by Equation 5.26. The initial condition is prescribed by Equation 5.27, and the interior boundary condition is of the form

$$T(x \rightarrow \infty, t) = T_i \quad (5.53)$$

Closed-form solutions have been obtained for three important surface conditions, instantaneously applied at  $t = 0$  [1, 2]. These conditions are shown in Figure 5.7. They include application of a constant surface temperature  $T_s \neq T_i$ , application of a constant surface heat flux  $q_o''$ , and exposure of the surface to a fluid characterized by  $T_\infty \neq T_i$  and the convection coefficient  $h$ .

The solution for case 1 may be obtained by recognizing the existence of a *similarity variable*  $\eta$ , through which the heat equation may be transformed from a partial differential equation, involving two independent variables ( $x$  and  $t$ ), to an ordinary differential equation expressed in terms of the single similarity variable. To confirm that such a requirement is satisfied by  $\eta \equiv x/(4\alpha t)^{1/2}$ , we first transform the pertinent differential operators, such that

$$\begin{aligned} \frac{\partial T}{\partial x} &= \frac{dT}{d\eta} \frac{\partial \eta}{\partial x} = \frac{1}{(4\alpha t)^{1/2}} \frac{dT}{d\eta} \\ \frac{\partial^2 T}{\partial x^2} &= \frac{d}{d\eta} \left[ \frac{\partial T}{\partial x} \right] \frac{\partial \eta}{\partial x} = \frac{1}{4\alpha t} \frac{d^2 T}{d\eta^2} \\ \frac{\partial T}{\partial t} &= \frac{dT}{d\eta} \frac{\partial \eta}{\partial t} = -\frac{x}{2t(4\alpha t)^{1/2}} \frac{dT}{d\eta} \end{aligned}$$

Substituting into Equation 5.26, the heat equation becomes

$$\frac{d^2 T}{d\eta^2} = -2\eta \frac{dT}{d\eta} \quad (5.54)$$

With  $x = 0$  corresponding to  $\eta = 0$ , the surface condition may be expressed as

$$T(\eta = 0) = T_s \quad (5.55)$$

and with  $x \rightarrow \infty$ , as well as  $t = 0$ , corresponding to  $\eta \rightarrow \infty$ , both the initial condition and the interior boundary condition correspond to the single requirement that

$$T(\eta \rightarrow \infty) = T_i \quad (5.56)$$

Since the transformed heat equation and the initial/boundary conditions are independent of  $x$  and  $t$ ,  $\eta \equiv x/(4\alpha t)^{1/2}$  is, indeed, a similarity variable. Its existence implies that, irrespective of the values of  $x$  and  $t$ , the temperature may be represented as a unique function of  $\eta$ .

The specific form of the temperature dependence,  $T(\eta)$ , may be obtained by separating variables in Equation 5.54, such that

$$\frac{d(dT/d\eta)}{(dT/d\eta)} = -2\eta \, d\eta$$

Integrating, it follows that

$$\ln(dT/d\eta) = -\eta^2 + C_1'$$

or

$$\frac{dT}{d\eta} = C_1 \exp(-\eta^2)$$

Integrating a second time, we obtain

$$T = C_1 \int_0^\eta \exp(-u^2) \, du + C_2$$

where  $u$  is a dummy variable. Applying the boundary condition at  $\eta = 0$ , Equation 5.55, it follows that  $C_2 = T_s$  and

$$T = C_1 \int_0^\eta \exp(-u^2) \, du + T_s$$

From the second boundary condition, Equation 5.56, we obtain

$$T_i = C_1 \int_0^\infty \exp(-u^2) \, du + T_s$$

or, evaluating the definite integral,

$$C_1 = \frac{2(T_i - T_s)}{\pi^{1/2}}$$

Hence the temperature distribution may be expressed as

$$\frac{T - T_s}{T_i - T_s} = (2/\pi^{1/2}) \int_0^\eta \exp(-u^2) \, du \equiv \text{erf } \eta \quad (5.57)$$

where the *Gaussian error function*,  $\text{erf } \eta$ , is a standard mathematical function that is tabulated in Appendix B. Note that  $\text{erf}(\eta)$  asymptotically approaches unity as  $\eta$  becomes infinite. Thus, at any nonzero time, temperatures everywhere are predicted to have changed from  $T_i$  (become closer to  $T_s$ ). The infinite speed at which

boundary-condition information propagates into the semi-infinite solid is physically unrealistic, but this limitation of Fourier's law is not important except at extremely small time scales, as discussed in Section 2.3. The surface heat flux may be obtained by applying Fourier's law at  $x = 0$ , in which case

$$\begin{aligned} q_s'' &= -k \frac{\partial T}{\partial x} \Big|_{x=0} = -k(T_i - T_s) \frac{d(\operatorname{erf} \eta)}{d\eta} \frac{\partial \eta}{\partial x} \Big|_{\eta=0} \\ q_s'' &= k(T_s - T_i)(2/\pi^{1/2})\exp(-\eta^2)(4\alpha t)^{-1/2} \Big|_{\eta=0} \\ q_s'' &= \frac{k(T_s - T_i)}{(\pi\alpha t)^{1/2}} \end{aligned} \quad (5.58)$$

Analytical solutions may also be obtained for the case 2 and case 3 surface conditions, and results for all three cases are summarized as follows.

**Case 1 Constant Surface Temperature:**  $T(0, t) = T_s$

$$\frac{T(x, t) - T_s}{T_i - T_s} = \operatorname{erf}\left(\frac{x}{2\sqrt{\alpha t}}\right) \quad (5.57)$$

$$q_s''(t) = \frac{k(T_s - T_i)}{\sqrt{\pi\alpha t}} \quad (5.58)$$

**Case 2 Constant Surface Heat Flux:**  $q_s'' = q_o''$

$$T(x, t) - T_i = \frac{2q_o''(\alpha t/\pi)^{1/2}}{k} \exp\left(\frac{-x^2}{4\alpha t}\right) - \frac{q_o'' x}{k} \operatorname{erfc}\left(\frac{x}{2\sqrt{\alpha t}}\right) \quad (5.59)$$

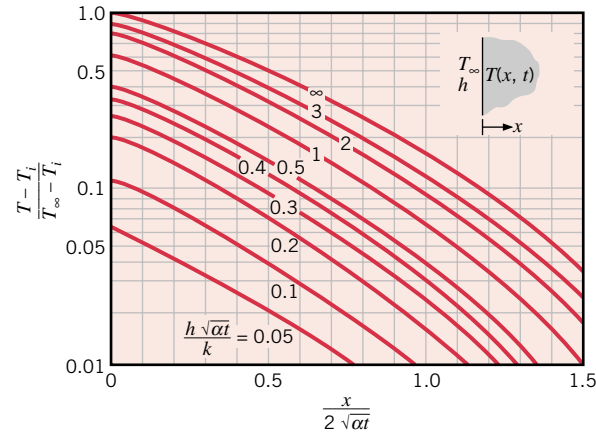
**Case 3 Surface Convection:**  $-k \frac{\partial T}{\partial x} \Big|_{x=0} = h[T_\infty - T(0, t)]$

$$\begin{aligned} \frac{T(x, t) - T_i}{T_\infty - T_i} &= \operatorname{erfc}\left(\frac{x}{2\sqrt{\alpha t}}\right) \\ &\quad - \left[ \exp\left(\frac{hx}{k} + \frac{h^2\alpha t}{k^2}\right) \right] \left[ \operatorname{erfc}\left(\frac{x}{2\sqrt{\alpha t}} + \frac{h\sqrt{\alpha t}}{k}\right) \right] \end{aligned} \quad (5.60)$$

The *complementary error function*,  $\operatorname{erfc} w$ , is defined as  $\operatorname{erfc} w \equiv 1 - \operatorname{erf} w$ .

Temperature histories for the three cases are shown in Figure 5.7, and distinguishing features should be noted. With a step change in the surface temperature, case 1, temperatures within the medium monotonically approach  $T_s$  with increasing  $t$ , while the magnitude of the surface temperature gradient, and hence the surface heat flux, decreases as  $t^{-1/2}$ . In contrast, for a fixed surface heat flux (case 2), Equation 5.59 reveals that  $T(0, t) = T_s(t)$  increases monotonically as  $t^{1/2}$ . For surface convection (case 3), the surface temperature and temperatures within the medium approach the fluid temperature  $T_\infty$  with increasing time. As  $T_s$  approaches  $T_\infty$ , there is, of course, a reduction in the surface heat flux,  $q_s''(t) = h[T_\infty - T_s(t)]$ . Specific temperature histories computed from Equation 5.60 are plotted in Figure 5.8. The result corresponding to  $h = \infty$  is equivalent to that associated with a sudden change



**FIGURE 5.8**

Temperature histories in a semi-infinite solid with surface convection [2]. Adapted with permission.

in surface temperature, case 1. That is, for  $h = \infty$ , the surface instantaneously achieves the imposed fluid temperature ( $T_s = T_\infty$ ), and with the second term on the right-hand side of Equation 5.60 reducing to zero, the result is equivalent to Equation 5.57.

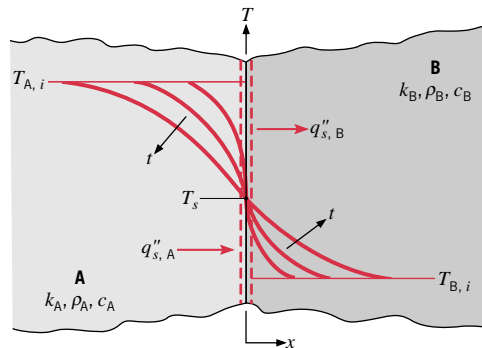
An interesting permutation of case 1 results when two semi-infinite solids, initially at uniform temperatures  $T_{A,i}$  and  $T_{B,i}$ , are placed in contact at their free surfaces (Figure 5.9). If the contact resistance is negligible, the requirement of thermal equilibrium dictates that, at the instant of contact ( $t = 0$ ), both surfaces must assume the same temperature  $T_s$ , for which  $T_{B,i} < T_s < T_{A,i}$ . Since  $T_s$  does not change with increasing time, it follows that the transient thermal response and the surface heat flux of each of the solids are determined by Equations 5.57 and 5.58, respectively.

The equilibrium surface temperature of Figure 5.9 may be determined from a surface energy balance, which requires that

$$q''_{s,A} = q''_{s,B} \quad (5.61)$$

Substituting from Equation 5.58 for  $q''_{s,A}$  and  $q''_{s,B}$  and recognizing that the  $x$  coordinate of Figure 5.9 requires a sign change for  $q''_{s,A}$ , it follows that

$$\frac{-k_A(T_s - T_{A,i})}{(\pi\alpha_A t)^{1/2}} = \frac{k_B(T_s - T_{B,i})}{(\pi\alpha_B t)^{1/2}} \quad (5.62)$$

**FIGURE 5.9**

Interfacial contact between two semi-infinite solids at different initial temperatures.

or, solving for  $T_s$ ,

$$T_s = \frac{(k\rho c)_A^{1/2} T_{A,i} + (k\rho c)_B^{1/2} T_{B,i}}{(k\rho c)_A^{1/2} + (k\rho c)_B^{1/2}} \quad (5.63)$$

Hence the quantity  $m \equiv (k\rho c)^{1/2}$  is a weighting factor that determines whether  $T_s$  will more closely approach  $T_{A,i}$  ( $m_A > m_B$ ) or  $T_{B,i}$  ( $m_B > m_A$ ).

### EXAMPLE 5.6

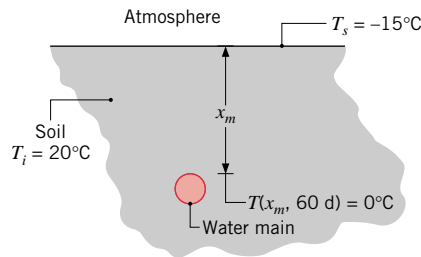
In laying water mains, utilities must be concerned with the possibility of freezing during cold periods. Although the problem of determining the temperature in soil as a function of time is complicated by changing surface conditions, reasonable estimates can be based on the assumption of a constant surface temperature over a prolonged period of cold weather. What minimum burial depth  $x_m$  would you recommend to avoid freezing under conditions for which soil, initially at a uniform temperature of  $20^\circ\text{C}$ , is subjected to a constant surface temperature of  $-15^\circ\text{C}$  for 60 days?

### SOLUTION

**Known:** Temperature imposed at the surface of soil initially at  $20^\circ\text{C}$ .

**Find:** The depth  $x_m$  to which the soil has frozen after 60 days.

**Schematic:**



**Assumptions:**

1. One-dimensional conduction in  $x$ .
2. Soil is a semi-infinite medium.
3. Constant properties.

**Properties:** Table A.3, soil (300 K):  $\rho = 2050 \text{ kg/m}^3$ ,  $k = 0.52 \text{ W/m} \cdot \text{K}$ ,  $c = 1840 \text{ J/kg} \cdot \text{K}$ ,  $\alpha = (k/\rho c) = 0.138 \times 10^{-6} \text{ m}^2/\text{s}$ .

**Analysis:** The prescribed conditions correspond to those of case 1 of Figure 5.7, and the transient temperature response of the soil is governed by Equation 5.57. Hence at the time  $t = 60$  days after the surface temperature change,

$$\frac{T(x_m, t) - T_s}{T_i - T_s} = \text{erf}\left(\frac{x_m}{2\sqrt{\alpha t}}\right)$$

or

$$\frac{0 - (-15)}{20 - (-15)} = 0.429 = \operatorname{erf}\left(\frac{x_m}{2\sqrt{\alpha t}}\right)$$

Hence, from Appendix B.2

$$\frac{x_m}{2\sqrt{\alpha t}} = 0.40$$

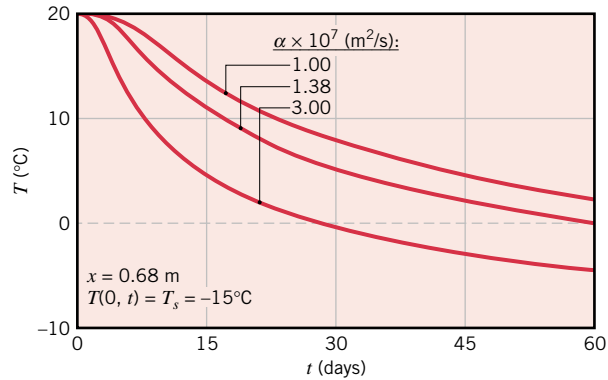
and

$$x_m = 0.80(\alpha t)^{1/2} = 0.80(0.138 \times 10^{-6} \text{ m}^2/\text{s} \times 60 \text{ days} \times 24 \text{ h/day} \times 3600 \text{ s/h})^{1/2} = 0.68 \text{ m}$$

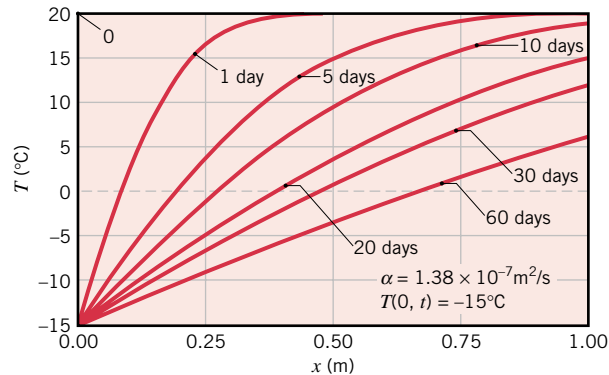
◁

### Comments:

1. The properties of soil are highly variable, depending on the nature of the soil and its moisture content, and a representative range of thermal diffusivities is  $1 \times 10^{-7} < \alpha < 3 \times 10^{-7} \text{ m}^2/\text{s}$ . To assess the effect of soil properties on freezing conditions, we use Equation 5.57 to compute temperature histories at  $x_m = 0.68 \text{ m}$  for  $\alpha \times 10^7 = 1.0, 1.38, \text{ and } 3.0 \text{ m}^2/\text{s}$ .



If  $\alpha > 1.38 \times 10^{-7} \text{ m}^2/\text{s}$ , the design criterion is not achieved at  $x_m = 0.68 \text{ m}$  and freezing would occur. It is also instructional to examine temperature distributions in the soil at representative times during the cooling period. Using Equation 5.57 with  $\alpha = 1.38 \times 10^{-7} \text{ m}^2/\text{s}$ , the following results are obtained:



As thermal penetration increases with increasing time, the temperature gradient at the surface,  $\partial T/\partial x|_{x=0}$ , and hence the rate of heat extraction from the soil, decreases.

2. The *IHT Models, Transient Conduction, Semi-infinite Solid* option may be used to generate the foregoing numerical results. The option provides model builders for the three boundary conditions of *constant surface temperature*, *constant surface heat flux*, and *surface convection*.

## 5.8

### Objects with Constant Surface Temperatures or Surface Heat Fluxes

In Sections 5.5 and 5.6, the transient thermal response of plane walls, cylinders, and spheres to an applied convection boundary condition was considered in detail. It was pointed out that the solutions in those sections may be used for cases involving a step change in surface temperature by allowing the Biot number to be infinite. In Section 5.7, the response of a semi-infinite solid to a step change in surface temperature, or to an applied constant heat flux, was determined. This section further explores the transient thermal response of a variety of objects to a constant surface temperature or a constant surface heat flux boundary condition.

#### 5.8.1 Constant Temperature Boundary Conditions

In the following discussion, the transient thermal response of objects to a step change in surface temperature is considered.

**Semi-Infinite Solid** Insight into the thermal response of objects to an applied constant temperature boundary condition may be obtained by casting the heat flux in Equation 5.58 into the nondimensional form

$$q^* \equiv \frac{q_s'' L_c}{k(T_s - T_i)} \quad (5.64)$$

where  $L_c$  is a *characteristic length* and  $q^*$  is the *dimensionless conduction heat rate* that was introduced in Section 4.3.3. Substituting Equation 5.64 into Equation 5.58 yields

$$q^* = \frac{1}{\sqrt{\pi Fo}} \quad (5.65)$$

where the Fourier number is defined as  $Fo \equiv \alpha t/L_c^2$ . Note that the value of  $q_s''$  is independent of the choice of the characteristic length, as it must be for a semi-infinite solid. Equation 5.65 is plotted in Figure 5.10a, and since  $q^* \propto Fo^{-1/2}$ , the slope of the line is  $-1/2$  on the log-log plot.

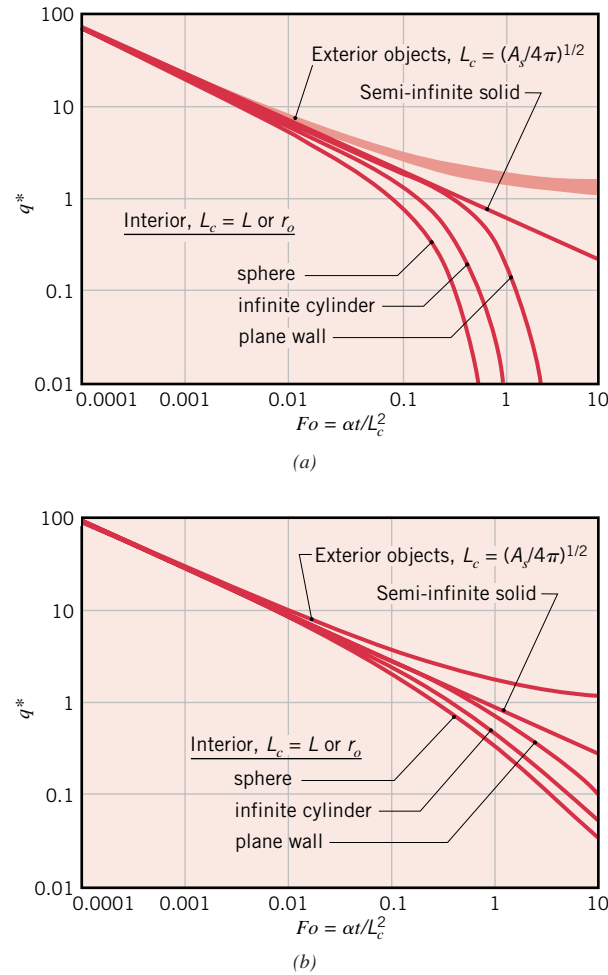


**FIGURE 5.10** Transient dimensionless conduction heat rates for a variety of geometries. (a) Constant surface temperature. Results for the geometries of Table 4.1 lie within the shaded region and are from [5]. (b) Constant surface heat flux.

**Interior Heat Transfer: Plane Wall, Cylinder, and Sphere** Results for heat transfer to the *interior* of a plane wall, cylinder, and sphere are also shown in Figure 5.10a. These results are generated by using Fourier's law in conjunction with Equations 5.39, 5.47, and 5.48 for  $Bi \rightarrow \infty$ . As in Sections 5.5 and 5.6, the characteristic length is  $L_c = L$  or  $r_o$  for a plane wall of thickness  $2L$  or a cylinder (or sphere) of radius  $r_o$ , respectively. For each geometry,  $q^*$  initially follows the semi-infinite solid solution but at some point decreases rapidly as the objects approach their equilibrium temperature and  $q_s''(t \rightarrow \infty) \rightarrow 0$ . The value of  $q^*$  is expected to decrease more rapidly for geometries that possess large surface area to volume ratios, and this trend is evident in Figure 5.10a.

**Exterior Heat Transfer: Various Geometries** Additional results are shown in Figure 5.10a for an object that is embedded in an exterior (surrounding) medium

of infinite extent. The infinite medium is initially at temperature  $T_i$ , and the surface temperature of the object is suddenly changed to  $T_s$ . For the exterior cases,  $L_c$  is the characteristic length used in Section 4.3.3, namely  $L_c = (A_s/4\pi)^{1/2}$ . For the sphere in a surrounding infinite medium, the exact solution for  $q^*(Fo)$  is [5]

$$q^* = \frac{1}{\sqrt{\pi Fo}} + 1 \quad (5.66)$$

As seen in the figure, for all of the *exterior cases*  $q^*$  closely mimics that of the sphere when the appropriate length scale is used in its definition, regardless of the object's shape. In a manner consistent with the interior cases,  $q^*$  initially follows the semi-infinite solid solution. In contrast to the interior cases,  $q^*$  eventually reaches the nonzero, steady-state value of  $q_{ss}^*$  that is listed in Table 4.1. Note that  $q_s''$  in Equation 5.64 is the *average* surface heat flux for geometries that have nonuniform surface heat flux.

As seen in Figure 5.10a, all of the thermal responses collapse to that of the semi-infinite solid for early times, that is, for  $Fo$  less than approximately  $10^{-3}$ . This remarkable consistency reflects the fact that temperature variations are confined to thin layers adjacent to the surface of any object at early times, regardless of whether internal or external heat transfer is of interest. At early times, therefore, Equations 5.57 and 5.58 may be used to predict the temperatures and heat transfer rates within the thin regions adjacent to the boundaries of any object. For example, predicted local heat fluxes and local dimensionless temperatures using the semi-infinite solid solutions are within approximately 5% of the predictions obtained from the exact solutions for the interior and exterior heat transfer cases involving spheres when  $Fo \leq 10^{-3}$ .

### 5.8.2 Constant Heat Flux Boundary Conditions

When a constant surface heat flux is applied to an object, the resulting surface temperature history is often of interest. In this case, the heat flux in the numerator of Equation 5.64 is now constant, and the temperature difference in the denominator,  $T_s - T_i$ , increases with time.

**Semi-Infinite Solid** In the case of a semi-infinite solid, the surface temperature history can be found by evaluating Equation 5.59 at  $x = 0$ , which may be re-arranged and combined with Equation 5.64 to yield

$$q^* = \frac{1}{2} \sqrt{\frac{\pi}{Fo}} \quad (5.67)$$

As for the constant temperature case,  $q^* \propto Fo^{-1/2}$ , but with a different coefficient. Equation 5.67 is presented in Figure 5.10b.

**Interior Heat Transfer: Plane Wall, Cylinder, and Sphere** A second set of results is shown in Figure 5.10b for the *interior* cases of the plane wall, cylinder, and sphere. As for the constant surface temperature results of Figure 5.10a,  $q^*$  initially follows the semi-infinite solid solution and subsequently decreases more rapidly, with the decrease occurring first for the sphere, then the cylinder, and finally the plane wall. Compared to the constant surface temperature case, the rate at which  $q^*$  decreases is not as dramatic, since steady-state conditions are never reached; the surface temperature must continue to increase with time. At *late* times (large  $Fo$ ), the surface temperature increases linearly with time, yielding  $q^* \propto Fo^{-1}$ , with a slope of  $-1$  on the log-log plot.

**Exterior Heat Transfer: Various Geometries** Results for heat transfer between a sphere and an exterior infinite medium are also presented in Figure 5.10b. The exact solution for the embedded sphere is

$$q^* = [1 - \exp(Fo) \operatorname{erfc}(Fo^{1/2})]^{-1} \quad (5.68)$$

As in the constant surface temperature case of Figure 5.10a, this solution approaches steady-state conditions, with  $q_{ss}^* = 1$ . For objects of other shapes that are embedded within an infinite medium,  $q^*$  would follow the semi-infinite solid solution at small  $Fo$ . At larger  $Fo$ ,  $q^*$  must asymptotically approach the value of  $q_{ss}^*$  given in Table 4.1 where  $T_s$  in Equation 5.64 is the *average* surface temperature for geometries that have nonuniform surface temperatures.

### 5.8.3 Approximate Solutions

Simple expressions have been developed for  $q^*(Fo)$ . These expressions may be used to approximate all the results included in Figure 5.10 over the *entire range of*  $Fo$ . These expressions are listed in Table 5.2, along with the corresponding exact solutions. Table 5.2a is for the constant surface temperature case, while Table 5.2b is for the constant surface heat flux situation. For each of the geometries listed in the left-hand column, the tables provide the length scale to be used in the definition of both  $Fo$  and  $q^*$ , the exact solution for  $q^*(Fo)$ , the approximation solutions for early times ( $Fo < 0.2$ ) and late times ( $Fo \geq 0.2$ ), and the maximum percentage error associated with use of the approximations (which occurs at  $Fo \approx 0.2$  for all results except the external sphere with constant heat flux).

#### EXAMPLE 5.7

A proposed cancer treatment utilizes small, composite *nanoshells* whose size and composition are carefully engineered so that the particles efficiently absorb laser irradiation at particular wavelengths [6]. Prior to treatment, antibodies are attached to the nanoscale particles. The doped particles are then injected into the patient's bloodstream and are distributed throughout the body. The antibodies are attracted to malignant sites, and therefore carry and adhere the nanoshells only to cancerous tissue. After the particles have come to rest within the tumor, a laser beam penetrates through the tissue between the skin and the cancer, is absorbed by the nanoshells, and, in turn, heats and destroys the cancerous tissues.

Consider an approximately spherical tumor of diameter  $D_t = 3$  mm that is uniformly infiltrated with nanoshells that are highly absorptive of incident radiation from a laser located outside the patient's body.

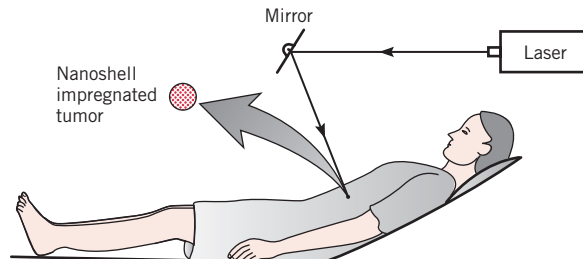


**TABLE 5.2a** Summary of transient heat transfer results for constant surface temperature cases<sup>a</sup>

Geometry	Length Scale, $L_c$	Exact Solutions	$q^*(Fo)$		Maximum Error (%)
			$Fo < 0.2$	$Fo \geq 0.2$	
Semi-infinite	$L$ (arbitrary)	$\frac{1}{\sqrt{\pi Fo}}$	Use exact solution.		none
Interior Cases					
Plane wall of thickness $2L$	$L$	$2 \sum_{n=1}^{\infty} \exp(-\xi_n^2 Fo) \quad \xi_n = (n - \frac{1}{2})\pi$	$\frac{1}{\sqrt{\pi Fo}}$	$2 \exp(-\xi_1^2 Fo) \quad \xi_1 = \pi/2$	1.7
Infinite cylinder	$r_o$	$2 \sum_{n=1}^{\infty} \exp(-\xi_n^2 Fo) \quad J_0(\xi_n) = 0$	$\frac{1}{\sqrt{\pi Fo}}$	$2 \exp(-\xi_1^2 Fo) \quad \xi_1 = 2.4050$	0.8
Sphere	$r_o$	$2 \sum_{n=1}^{\infty} \exp(-\xi_n^2 Fo) \quad \xi_n = n\pi$	$\frac{1}{\sqrt{\pi Fo}}$	$2 \exp(-\xi_1^2 Fo) \quad \xi_1 = \pi$	6.3
Exterior Cases					
Sphere	$r_o$	$\frac{1}{\sqrt{\pi Fo}} + 1$	Use exact solution.		none
Various shapes (Table 4.1, cases 12–15)	$(A_s/4\pi)^{1/2}$	none	$\frac{1}{\sqrt{\pi Fo}} + q_s^*, \quad q_s^*$ from Table 4.1		7.1

<sup>a</sup> $q^* \equiv q'' L_c / k(T_s - T_i)$  and  $Fo \equiv \alpha t / L_c^2$  where  $L_c$  is the length scale given in the table,  $T_s$  is the object surface temperature, and  $T_i$  is (a) the initial object temperature for the interior cases and (b) the temperature of the infinite medium for the exterior cases.



**TABLE 5.2b** Summary of transient heat transfer results for constant surface heat flux cases<sup>a</sup>

Geometry	Length Scale, $L_c$	Exact Solutions	$q^*(Fo)$		Maximum Error (%)
			Approximate Solutions		
			$Fo < 0.2$	$Fo \geq 0.2$	
Semi-infinite	$L$ (arbitrary)	$\frac{1}{2}\sqrt{\frac{\pi}{Fo}}$	Use exact solution.		none
<b>Interior Cases</b>					
Plane wall of thickness $2L$	$L$	$\left[Fo + \frac{1}{3} - 2\sum_{n=1}^{\infty}\frac{\exp(-\xi_n^2 Fo)}{\xi_n^2}\right]^{-1}$	$\xi_n = n\pi$	$\left[Fo + \frac{1}{3}\right]^{-1}$	5.3
Infinite cylinder	$r_o$	$\left[2Fo + \frac{1}{4} - 2\sum_{n=1}^{\infty}\frac{\exp(-\xi_n^2 Fo)}{\xi_n^2}\right]^{-1}$	$J_1(\xi_n) = 0$	$\left[2Fo + \frac{1}{4}\right]^{-1}$	2.1
Sphere	$r_o$	$\left[3Fo + \frac{1}{5} - 2\sum_{n=1}^{\infty}\frac{\exp(-\xi_n^2 Fo)}{\xi_n^2}\right]^{-1}$	$\tan(\xi_n) = \xi_n$	$\left[3Fo + \frac{1}{5}\right]^{-1}$	4.5
<b>Exterior Cases</b>					
Sphere	$r_o$	$[1 - \exp(Fo)\text{erfc}(Fo^{1/2})]^{-1}$	$\frac{1}{2}\sqrt{\frac{\pi}{Fo}} + \frac{\pi}{4}$	$\frac{0.77}{\sqrt{Fo}} + 1$	3.2
Various shapes (Table 4.1, cases 12–15)	$(A_s/4\pi)^{1/2}$	none	$\frac{1}{2}\sqrt{\frac{\pi}{Fo}} + \frac{\pi}{4}$	$\frac{0.77}{\sqrt{Fo}} + q_{ss}^*$	unknown

<sup>a</sup> $q^* \equiv q_s'' L_c / k(T_s - T_i)$  and  $Fo \equiv \alpha t / L_c^2$  where  $L_c$  is the length scale given in the table,  $T_s$  is the object surface temperature, and  $T_i$  is (a) the initial object temperature for the interior cases and (b) the temperature of the infinite medium for the exterior cases.

1. Estimate the heat transfer rate from the tumor to the surrounding healthy tissue for a steady-state treatment temperature of  $T_{t,ss} = 55^\circ\text{C}$  at the surface of the tumor. The thermal conductivity of healthy tissue is approximately  $k = 0.5 \text{ W/m} \cdot \text{K}$ , and the body temperature is  $T_b = 37^\circ\text{C}$ .
2. Find the laser power necessary to sustain the tumor surface temperature at  $T_{t,ss} = 55^\circ\text{C}$  if the tumor is located  $d = 20 \text{ mm}$  beneath the surface of the skin, and the laser heat flux decays exponentially,  $q''_l(x) = q''_{l,o}(1 - \rho)e^{-\kappa x}$ , between the surface of the body and the tumor. In the preceding expression,  $q''_{l,o}$  is the laser heat flux outside the body,  $\rho = 0.05$  is the reflectivity of the skin surface, and  $\kappa = 0.02 \text{ mm}^{-1}$  is the *extinction coefficient* of the tissue between the tumor and the surface of the skin. The laser beam has a diameter of  $D_l = 5 \text{ mm}$ .
3. Neglecting heat transfer to the surrounding tissue, estimate the time at which the tumor temperature is within  $3^\circ\text{C}$  of  $T_{t,ss} = 55^\circ\text{C}$  for the laser power found in part 2. Assume the tissue's density and specific heat are that of water.
4. Neglecting the thermal mass of the tumor but accounting for heat transfer to the surrounding tissue, estimate the time needed for the surface temperature of the tumor to reach  $T_t = 52^\circ\text{C}$ .

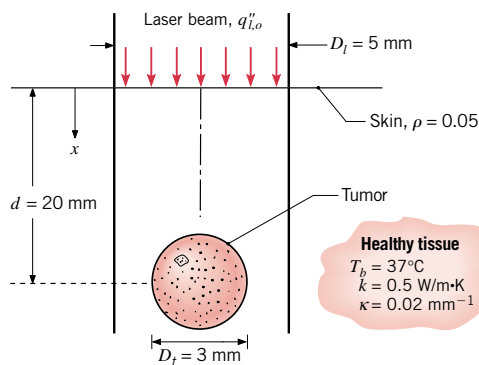
### SOLUTION

**Known:** Size of a small sphere; thermal conductivity, reflectivity, and extinction coefficient of tissue; depth of sphere below the surface of the skin.

### Find:

1. Heat transferred from the tumor to maintain its surface temperature at  $T_{t,ss} = 55^\circ\text{C}$ .
2. Laser power needed to sustain the tumor surface temperature at  $T_{t,ss} = 55^\circ\text{C}$ .
3. Time for the tumor to reach  $T_t = 52^\circ\text{C}$  when heat transfer to the surrounding tissue is neglected.
4. Time for the tumor to reach  $T_t = 52^\circ\text{C}$  when heat transfer to the surrounding tissue is considered and the thermal mass of the tumor is neglected.

### Schematic:



**Assumptions:**

1. One-dimensional conduction in the radial direction.
2. Constant properties.
3. Healthy tissue can be treated as an infinite medium.
4. The treated tumor absorbs all irradiation incident from the laser.
5. Lumped capacitance behavior for the tumor.
6. Neglect potential nanoscale heat transfer effects.
7. Neglect the effect of perfusion.

**Properties:** Table A.6, water (320 K, assumed):  $\rho = v_f^{-1} = 989.1 \text{ kg/m}^3$ ,  $c_p = 4180 \text{ J/kg} \cdot \text{K}$ .

**Analysis:**

1. The steady-state heat loss from the spherical tumor may be determined by evaluating the dimensionless heat rate from the expression for case 12 of Table 4.1:

$$q = 2\pi k D_i (T_{t,ss} - T_b) = 2 \times \pi \times 0.5 \text{ W/m} \cdot \text{K} \times 3 \times 10^{-3} \text{ m} \times (55 - 37)^\circ\text{C} = 0.170 \text{ W} \quad \triangleleft$$

2. The laser irradiation will be absorbed over the projected area of the tumor,  $\pi D_i^2/4$ . To determine the laser power corresponding to  $q = 0.170 \text{ W}$ , we first write an energy balance for the sphere. For a control surface about the sphere, the energy absorbed from the laser irradiation is offset by heat conduction to the healthy tissue,  $q = 0.170 \text{ W} \approx q_i''(x = d)\pi D_i^2/4$ , where,  $q_i''(x = d) = q_{i,o}''(1 - \rho)e^{-\kappa d}$  and the laser power is  $P_l = q_{i,o}''\pi D_i^2/4$ . Hence,

$$\begin{aligned} P_l &= q D_i^2 e^{\kappa d} / [(1 - \rho) D_i^2] \\ &= 0.170 \text{ W} \times (5 \times 10^{-3} \text{ m})^2 \times e^{(0.02 \text{ mm}^{-1} \times 20 \text{ mm})} / [(1 - 0.05) \times (3 \times 10^{-3} \text{ m})^2] \\ &= 0.74 \text{ W} \quad \triangleleft \end{aligned}$$

3. The general lumped capacitance energy balance, Equation 5.14, may be written

$$q_i''(x = d)\pi D_i^2/4 = q = \rho V c \frac{dT}{dt}$$

Separating variables and integrating between appropriate limits,

$$\frac{q}{\rho V c} \int_{t=0}^t dt = \int_{T_b}^{T_i} dT$$

yields

$$\begin{aligned} t &= \frac{\rho V c}{q} (T_i - T_b) = \frac{989.1 \text{ kg/m}^3 \times (\pi/6) \times (3 \times 10^{-3} \text{ m})^3 \times 4180 \text{ J/kg} \cdot \text{K}}{0.170 \text{ W}} \\ &\quad \times (52^\circ\text{C} - 37^\circ\text{C}) \end{aligned}$$

or

$$t = 5.16 \text{ s} \quad \triangleleft$$

4. Using Equation 5.68,

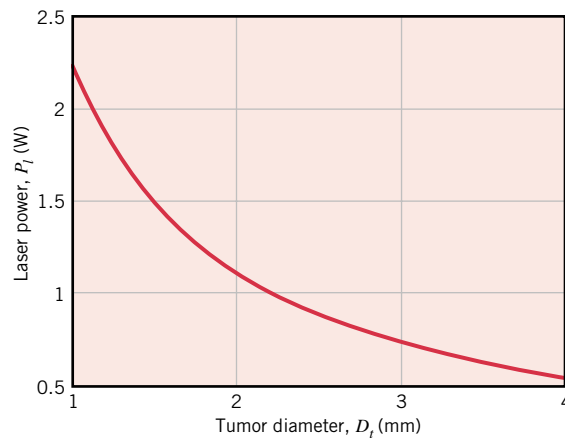
$$q/2\pi kD_i(T_i - T_b) = q^* = [1 - \exp(Fo)\operatorname{erfc}(Fo^{1/2})]^{-1}$$

which may be solved by trial-and-error to yield  $Fo = 10.3 = 4\alpha t/D_i^2$ . Then, with  $\alpha = k/\rho c = 0.50 \text{ W/m} \cdot \text{K}/(989.1 \text{ kg/m}^3 \times 4180 \text{ J/kg} \cdot \text{K}) = 1.21 \times 10^{-7} \text{ m}^2/\text{s}$ , we find

$$t = FoD_i^2/4\alpha = 10.3 \times (3 \times 10^{-3} \text{ m})^2/(4 \times 1.21 \times 10^{-7} \text{ m}^2/\text{s}) = 192 \text{ s} \quad \triangleleft$$

**Comments:**

1. The analysis does not account for blood perfusion. The flow of blood would lead to advection of warmed fluid away from the tumor (and relatively cool blood to the vicinity of the tumor), increasing the power needed to reach the desired treatment temperature.
2. The laser power needed to treat various-sized tumors, calculated as in parts 1 and 2 of the problem solution, is shown below. Note that as the tumor becomes smaller, a higher-powered laser is needed, which may seem counterintuitive. The power required to heat the tumor, which is the same as the heat loss calculated in part 1, increases in direct proportion to the diameter, as might be expected. However, since the laser power flux remains constant, a smaller tumor cannot absorb as much energy (the energy absorbed has a  $D_i^2$  dependence). Less of the overall laser power is utilized to heat the tumor, and the required laser power increases for smaller tumors.



3. To determine the *actual* time needed for the tumor temperature to approach steady-state conditions, a numerical solution of the heat diffusion equation applied to the surrounding tissue, *coupled* with a solution for the temperature history within the tumor, would be required. However, we see that significantly more time is needed for the surrounding tissue to reach steady-state conditions than to increase the temperature of the isolated spherical tumor. This is due to the fact that higher temperatures propagate into a large volume when heating of the surrounding tissue is considered, while in contrast the thermal mass of the tumor is limited by the tumor's size. Hence, the *actual* time to heat *both* the tumor and the surrounding tissue will be slightly greater than 192 s.

4. Since temperatures are likely to increase at a considerable distance from the tumor, the assumption that the surroundings are of infinite size would need to be checked by inspecting results of the proposed numerical solution described in Comment 3.

## 5.9

### Periodic Heating

*Periodic heating* is used in various applications, such as thermal processing of materials using pulsed lasers, and occurs naturally in situations such as those involving the collection of solar energy.

Consider, for example, the semi-infinite solid of Figure 5.11a. For a surface temperature history described by  $T(0,t) = T_i + \Delta T \sin \omega t$ , the solution of Equation 5.26 subject to the interior boundary condition given by Equation 5.53 is

$$\frac{T(x,t) - T_i}{\Delta T} = \exp[-x\sqrt{\omega/2\alpha}] \sin[\omega t - x\sqrt{\omega/2\alpha}] \quad (5.69)$$

This solution applies after sufficient time has passed to yield a *quasi* steady state for which all temperatures fluctuate periodically about a time-invariant mean value. At locations in the solid, the fluctuations have a time lag relative to the surface temperature. In addition, the amplitude of the fluctuations within the material decays exponentially with distance from the surface. For  $x > \delta_p \equiv 4\sqrt{\alpha/\omega}$ , the amplitude of the temperature fluctuation is reduced by approximately 90% relative to that of the surface. The term  $\delta_p$  is a *thermal penetration depth*, which is an indication of the extent to which significant temperature effects propagate within a medium. The heat flux at the surface may be determined by applying Fourier's law at  $x = 0$ , yielding

$$q_s''(t) = k\Delta T\sqrt{\omega/\alpha} \sin(\omega t + \pi/4) \quad (5.70)$$

Equation 5.70 reveals that the surface heat flux is periodic, with a time-averaged value of zero.

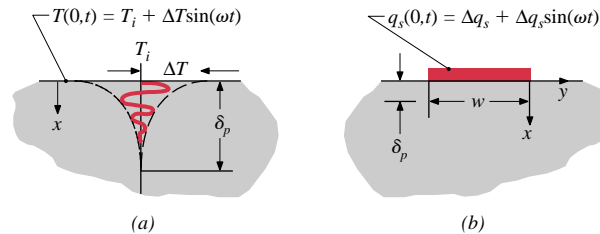


**FIGURE 5.11** Schematic of (a) a periodically heated, one-dimensional semi-infinite solid and (b) a periodically heated strip attached to a semi-infinite solid.

Periodic heating can also occur in two- or three-dimensional arrangements, as shown in Figure 5.11*b*. Recall that for this geometry, a steady state can be attained with constant heating of the strip placed upon a semi-infinite solid (Table 4.1, case 13). In a similar manner, a quasi steady state may be achieved when sinusoidal heating ( $q_s = \Delta q_s + \Delta q_s \sin \omega t$ ) is applied to the strip. Again, a quasi steady state is achieved for which all temperatures fluctuate about a time-invariant mean value.

The solution of the two-dimensional, transient heat diffusion equation for the two-dimensional configuration shown in Figure 5.11*b* has been obtained, and the relationship between the amplitude of the applied sinusoidal heating and the amplitude of the temperature response of the heated strip can be approximated as [7]

$$\Delta T \approx \frac{\Delta q_s}{L\pi k} \left[ -\frac{1}{2} \ln(\omega/2) - \ln(w^2/4\alpha) + C_1 \right] = \frac{\Delta q_s}{L\pi k} \left[ -\frac{1}{2} \ln(\omega/2) + C_2 \right] \quad (5.71)$$

where the constant  $C_1$  depends on the thermal contact resistance at the interface between the heated strip and the underlying material. Note that the amplitude of the temperature fluctuation,  $\Delta T$ , corresponds to the spatially averaged temperature of the rectangular strip of length  $L$  and width  $w$ . The heat flux from the strip to the semi-infinite medium is assumed to be spatially uniform. The approximation is valid for  $L \gg w$ . For the system of Figure 5.11*b*, the thermal penetration depth is smaller than that of Figure 5.11*a* because of the lateral spreading of thermal energy and is  $\delta_p \approx \sqrt{\alpha/\omega}$ .

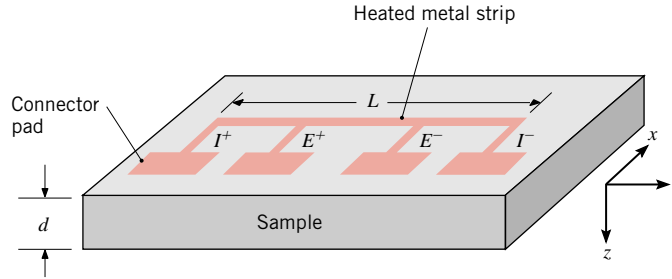
### EXAMPLE 5.8

A novel nanostructured dielectric material has been fabricated, and the following method is used to measure its thermal conductivity. A long metal strip 3000 angstroms thick,  $w = 100 \mu\text{m}$  wide, and  $L = 3.5 \text{ mm}$  long is deposited by a photolithography technique on the top surface of a  $d = 300\text{-}\mu\text{m}$  thick sample of the new material. The strip is heated periodically by an electric current supplied through two connector pads. The heating rate is  $q_s(t) = \Delta q_s + \Delta q_s \sin(\omega t)$ , where  $\Delta q_s$  is 3.5 mW. The instantaneous, spatially averaged temperature of the metal strip is found experimentally by measuring the time variation of its electrical resistance,  $R(t) = E(t)/I(t)$ , and by knowing how the electrical resistance of the metal varies with temperature. The measured temperature of the metal strip is periodic; it has an amplitude of  $\Delta T = 1.37 \text{ K}$  at a relatively low heating frequency of  $\omega = 2\pi \text{ rad/s}$  and 0.71 K at a frequency of  $200\pi \text{ rad/s}$ . Determine the thermal conductivity of the nanostructured dielectric material. The density and specific heats of the conventional version of the material are  $3100 \text{ kg/m}^3$  and  $820 \text{ J/kg} \cdot \text{K}$ , respectively.

### SOLUTION

**Known:** Dimensions of a thin metal strip, the frequency and amplitude of the electric power dissipated within the strip, the amplitude of the induced oscillating strip temperature, and the thickness of the underlying nanostructured material.

**Find:** The thermal conductivity of the nanostructured material.

**Schematic:****Assumptions:**

1. Two-dimensional transient conduction in the  $x$ - and  $z$ -directions.
2. Constant properties.
3. Negligible radiation and convection losses from the metal strip and top surface of the sample.
4. The nanostructured material sample is a semi-infinite solid.
5. Uniform heat flux at the interface between the heated strip and the nanostructured material.

**Analysis:** Substitution of  $\Delta T = 1.37$  K at  $\omega = 2\pi$  rad/s and  $\Delta T = 0.71$  K at  $\omega = 200\pi$  rad/s into Equation 5.71 results in two equations that may be solved simultaneously to yield

$$C_2 = 5.35 \quad k = 1.11 \text{ W/m} \cdot \text{K}$$


The thermal diffusivity is  $\alpha = 4.37 \times 10^{-7} \text{ m}^2/\text{s}$ , while the thermal penetration depths are estimated by  $\delta_p \approx \sqrt{\alpha/\omega}$ , resulting in  $\delta_p = 260 \text{ } \mu\text{m}$  and  $\delta_p = 26 \text{ } \mu\text{m}$  at  $\omega = 2\pi$  rad/s and  $\omega = 200\pi$  rad/s, respectively.

**Comments:**

1. The foregoing experimental technique, which is widely used to measure the thermal conductivity of microscale devices and nanostructured materials, is referred to as the *3  $\omega$  method* [7].
2. Because this technique is based on measurement of a temperature that fluctuates about a mean value that is approximately the same as the temperature of the surroundings, the measured value of  $k$  is relatively insensitive to radiation heat transfer losses from the top of the metal strip. Likewise, the technique is insensitive to thermal contact resistances that may exist at the interface between the sensing strip and the underlying material since these effects cancel when measurements are made at two different excitation frequencies [7].
3. The specific heat and density are not strongly dependent on the nanostructure of most solids, and properties of conventional material may be used.
4. The thermal penetration depth is less than the sample thickness. Therefore, treating the sample as a semi-infinite solid is a valid approach. Thinner samples could be used if higher heating frequencies were employed.

## 5.10

### Finite-Difference Methods

 Analytical solutions for some simple two- and three-dimensional geometries are found in Section 5S.2.

Analytical solutions to transient problems are restricted to simple geometries and boundary conditions, such as the one-dimensional cases considered in the preceding sections. For some simple two- and three-dimensional geometries, analytical solutions are still possible. However, in many cases the geometry and/or boundary conditions preclude the use of analytical techniques, and recourse must be made to *finite-difference* (or *finite-element*) methods. Such methods, introduced in Section 4.4 for steady-state conditions, are readily extended to transient problems. In this section we consider *explicit* and *implicit* forms of finite-difference solutions to transient conduction problems.

#### 5.10.1 Discretization of the Heat Equation: The Explicit Method

Once again consider the two-dimensional system of Figure 4.4. Under transient conditions with constant properties and no internal generation, the appropriate form of the heat equation, Equation 2.19, is

$$\frac{1}{\alpha} \frac{\partial T}{\partial t} = \frac{\partial^2 T}{\partial x^2} + \frac{\partial^2 T}{\partial y^2} \quad (5.72)$$

To obtain the finite-difference form of this equation, we may use the *central-difference* approximations to the spatial derivatives prescribed by Equations 4.27 and 4.28. Once again the  $m$  and  $n$  subscripts may be used to designate the  $x$  and  $y$  locations of *discrete nodal points*. However, in addition to being discretized in space, the problem must be discretized in time. The integer  $p$  is introduced for this purpose, where

$$t = p \Delta t \quad (5.73)$$

and the finite-difference approximation to the time derivative in Equation 5.72 is expressed as

$$\left. \frac{\partial T}{\partial t} \right|_{m,n} \approx \frac{T_{m,n}^{p+1} - T_{m,n}^p}{\Delta t} \quad (5.74)$$

The superscript  $p$  is used to denote the time dependence of  $T$ , and the time derivative is expressed in terms of the difference in temperatures associated with the *new* ( $p + 1$ ) and *previous* ( $p$ ) times. Hence calculations must be performed at successive times separated by the interval  $\Delta t$ , and just as a finite-difference solution restricts temperature determination to discrete points in space, it also restricts it to discrete points in time.

If Equation 5.74 is substituted into Equation 5.72, the nature of the finite-difference solution will depend on the specific time at which temperatures are evaluated in the finite-difference approximations to the spatial derivatives. In the *explicit method* of solution, these temperatures are evaluated at the *previous* ( $p$ ) time. Hence Equation 5.74 is considered to be a *forward-difference* approximation to the time derivative.



Evaluating terms on the right-hand side of Equations 4.27 and 4.28 at  $p$  and substituting into Equation 5.72, the explicit form of the finite-difference equation for the interior node  $m, n$  is

$$\frac{1}{\alpha} \frac{T_{m,n}^{p+1} - T_{m,n}^p}{\Delta t} = \frac{T_{m+1,n}^p + T_{m-1,n}^p - 2T_{m,n}^p}{(\Delta x)^2} + \frac{T_{m,n+1}^p + T_{m,n-1}^p - 2T_{m,n}^p}{(\Delta y)^2} \quad (5.75)$$

Solving for the nodal temperature at the new  $(p + 1)$  time and assuming that  $\Delta x = \Delta y$ , it follows that

$$T_{m,n}^{p+1} = Fo(T_{m+1,n}^p + T_{m-1,n}^p + T_{m,n+1}^p + T_{m,n-1}^p) + (1 - 4Fo)T_{m,n}^p \quad (5.76)$$

where  $Fo$  is a finite-difference form of the Fourier number

$$Fo = \frac{\alpha \Delta t}{(\Delta x)^2} \quad (5.77)$$

This approach can easily be extended to one- or three-dimensional systems. If the system is one-dimensional in  $x$ , the explicit form of the finite-difference equation for an interior node  $m$  reduces to

$$T_m^{p+1} = Fo(T_{m+1}^p + T_{m-1}^p) + (1 - 2Fo)T_m^p \quad (5.78)$$

Equations 5.76 and 5.78 are *explicit* because *unknown* nodal temperatures for the new time are determined exclusively by *known* nodal temperatures at the previous time. Hence calculation of the unknown temperatures is straightforward. Since the temperature of each interior node is known at  $t = 0$  ( $p = 0$ ) from prescribed initial conditions, the calculations begin at  $t = \Delta t$  ( $p = 1$ ), where Equation 5.76 or 5.78 is applied to each interior node to determine its temperature. With temperatures known for  $t = \Delta t$ , the appropriate finite-difference equation is then applied at each node to determine its temperature at  $t = 2 \Delta t$  ( $p = 2$ ). In this way, the transient temperature distribution is obtained by *marching out in time*, using intervals of  $\Delta t$ .

The accuracy of the finite-difference solution may be improved by decreasing the values of  $\Delta x$  and  $\Delta t$ . Of course, the number of interior nodal points that must be considered increases with decreasing  $\Delta x$ , and the number of time intervals required to carry the solution to a prescribed final time increases with decreasing  $\Delta t$ . Hence the computation time increases with decreasing  $\Delta x$  and  $\Delta t$ . The choice of  $\Delta x$  is typically based on a compromise between accuracy and computational requirements. Once this selection has been made, however, the value of  $\Delta t$  may not be chosen independently. It is, instead, determined by *stability* requirements.

An undesirable feature of the explicit method is that it is not unconditionally *stable*. In a transient problem, the solution for the nodal temperatures should continuously approach final (steady-state) values with increasing time. However, with the explicit method, this solution may be characterized by numerically induced oscillations, which are physically impossible. The oscillations may become *unstable*, causing the solution to diverge from the actual steady-state conditions. To prevent such erroneous results, the prescribed value of  $\Delta t$  must be maintained below a certain limit, which depends on  $\Delta x$  and other parameters of the system. This dependence is termed a *stability criterion*, which may be obtained mathematically or demonstrated from a thermodynamic argument (see Problem 5.92). For the problems of interest in this text, *the criterion is determined by requiring that the coefficient associated with the node of interest at the previous*

time is greater than or equal to zero. In general, this is done by collecting all terms involving  $T_{m,n}^p$  to obtain the form of the coefficient. This result is then used to obtain a limiting relation involving  $Fo$ , from which the maximum allowable value of  $\Delta t$  may be determined. For example, with Equations 5.76 and 5.78 already expressed in the desired form, it follows that the stability criterion for a one-dimensional interior node is  $(1 - 2Fo) \geq 0$ , or

$$Fo \leq \frac{1}{2} \quad (5.79)$$

and for a two-dimensional node, it is  $(1 - 4Fo) \geq 0$ , or

$$Fo \leq \frac{1}{4} \quad (5.80)$$

For prescribed values of  $\Delta x$  and  $\alpha$ , these criteria may be used to determine upper limits to the value of  $\Delta t$ .

Equations 5.76 and 5.78 may also be derived by applying the energy balance method of Section 4.4.3 to a control volume about the interior node. Accounting for changes in thermal energy storage, a general form of the energy balance equation may be expressed as

$$\dot{E}_{\text{in}} + \dot{E}_g = \dot{E}_{\text{st}} \quad (5.81)$$

In the interest of adopting a consistent methodology, it is again assumed that all heat flow is *into* the node.

To illustrate application of Equation 5.81, consider the surface node of the one-dimensional system shown in Figure 5.12. To more accurately determine thermal conditions near the surface, this node has been assigned a thickness that is one-half that of the interior nodes. Assuming convection transfer from an adjoining fluid and no generation, it follows from Equation 5.81 that

$$hA(T_{\infty} - T_0^p) + \frac{kA}{\Delta x}(T_1^p - T_0^p) = \rho cA \frac{\Delta x}{2} \frac{T_0^{p+1} - T_0^p}{\Delta t}$$

or, solving for the surface temperature at  $t + \Delta t$ ,

$$T_0^{p+1} = \frac{2h \Delta t}{\rho c \Delta x}(T_{\infty} - T_0^p) + \frac{2\alpha \Delta t}{\Delta x^2}(T_1^p - T_0^p) + T_0^p$$

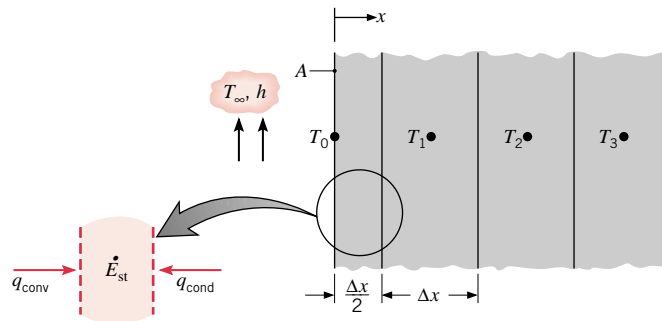


FIGURE 5.12 Surface node with convection and one-dimensional transient conduction.

Recognizing that  $(2h \Delta t / \rho c \Delta x) = 2(h \Delta x / k)(\alpha \Delta t / \Delta x^2) = 2 Bi Fo$  and grouping terms involving  $T_0^p$ , it follows that

$$T_0^{p+1} = 2Fo(T_1^p + Bi T_\infty) + (1 - 2Fo - 2Bi Fo)T_0^p \quad (5.82)$$

The finite-difference form of the Biot number is

$$Bi = \frac{h \Delta x}{k} \quad (5.83)$$

Recalling the procedure for determining the stability criterion, we require that the coefficient for  $T_0^p$  be greater than or equal to zero. Hence

$$1 - 2Fo - 2Bi Fo \geq 0$$

or

$$Fo(1 + Bi) \leq \frac{1}{2} \quad (5.84)$$

Since the complete finite-difference solution requires the use of Equation 5.78 for the interior nodes, as well as Equation 5.82 for the surface node, Equation 5.84 must be contrasted with Equation 5.79 to determine which requirement is more stringent. Since  $Bi \geq 0$ , it is apparent that the limiting value of  $Fo$  for Equation 5.84 is less than that for Equation 5.79. To ensure stability for all nodes, Equation 5.84 should therefore be used to select the maximum allowable value of  $Fo$ , and hence  $\Delta t$ , to be used in the calculations.

Forms of the explicit finite-difference equation for several common geometries are presented in Table 5.3(a). Each equation may be derived by applying the energy balance method to a control volume about the corresponding node. To develop confidence in your ability to apply this method, you should attempt to verify at least one of these equations.

### EXAMPLE 5.9

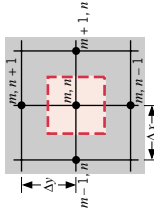
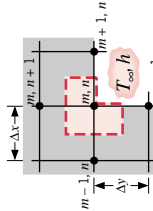
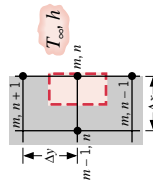
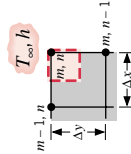
A fuel element of a nuclear reactor is in the shape of a plane wall of thickness  $2L = 20$  mm and is convectively cooled at both surfaces, with  $h = 1100$  W/m<sup>2</sup> · K and  $T_\infty = 250^\circ\text{C}$ . At normal operating power, heat is generated uniformly within the element at a volumetric rate of  $\dot{q}_1 = 10^7$  W/m<sup>3</sup>. A departure from the steady-state conditions associated with normal operation will occur if there is a change in the generation rate. Consider a sudden change to  $\dot{q}_2 = 2 \times 10^7$  W/m<sup>3</sup>, and use the explicit finite-difference method to determine the fuel element temperature distribution after 1.5 s. The fuel element thermal properties are  $k = 30$  W/m · K and  $\alpha = 5 \times 10^{-6}$  m<sup>2</sup>/s.

### SOLUTION

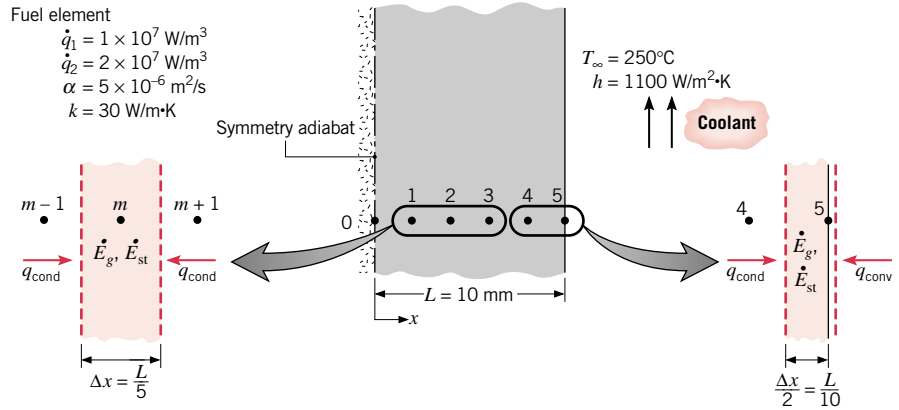
**Known:** Conditions associated with heat generation in a rectangular fuel element with surface cooling.

**Find:** Temperature distribution 1.5 s after a change in operating power.

**TABLE 5.3** Transient, two-dimensional finite-difference equations ( $\Delta x = \Delta y$ )

Configuration	(a) Explicit Method		(b) Implicit Method	
	Finite-Difference Equation	Stability Criterion		
	$T_{m,n}^{p+1} = Fo(T_{m+1,n}^p + T_{m-1,n}^p + T_{m,n+1}^p + T_{m,n-1}^p) + (1 - 4Fo)T_{m,n}^p$	$Fo \leq \frac{1}{4}$	$(1 + 4Fo)T_{m,n}^{p+1} - Fo(T_{m+1,n}^{p+1} + T_{m-1,n}^{p+1} + T_{m,n+1}^{p+1} + T_{m,n-1}^{p+1}) = T_{m,n}^p$	$(5.92)$
	1. Interior node	$(5.76)$		
	$T_{m,n}^{p+1} = \frac{2}{3}Fo(T_{m+1,n}^p + 2T_{m-1,n}^p + 2T_{m,n+1}^p + 2Bi T_{\infty}) + (1 - 4Fo - \frac{4}{3}Bi Fo)T_{m,n}^p$	$Fo(3 + Bi) \leq \frac{3}{4}$	$(1 + 4Fo(1 + \frac{1}{3}Bi))T_{m,n}^{p+1} - \frac{2}{3}Fo \cdot (T_{m+1,n}^{p+1} + 2T_{m-1,n}^{p+1} + 2T_{m,n+1}^{p+1} + T_{m,n-1}^{p+1}) = T_{m,n}^p + \frac{4}{3}Bi Fo T_{\infty}$	$(5.86)$ $(5.95)$
	2. Node at interior corner with convection	$(5.85)$		
	$T_{m,n}^{p+1} = Fo(2T_{m-1,n}^p + T_{m,n+1}^p + T_{m,n-1}^p + 2Bi T_{\infty}) + (1 - 4Fo - 2Bi Fo)T_{m,n}^p$	$Fo(2 + Bi) \leq \frac{1}{2}$	$(1 + 2Fo(2 + Bi))T_{m,n}^{p+1} - Fo(2T_{m-1,n}^{p+1} + T_{m,n+1}^{p+1} + T_{m,n-1}^{p+1} + 2Bi T_{\infty}) = T_{m,n}^p + 2Bi Fo T_{\infty}$	$(5.87)$ $(5.96)$
	3. Node at plane surface with convection <sup>a</sup>			
	$T_{m,n}^{p+1} = 2Fo(T_{m-1,n}^p + T_{m,n-1}^p + 2Bi T_{\infty}) + (1 - 4Fo - 4Bi Fo)T_{m,n}^p$	$Fo(1 + Bi) \leq \frac{1}{4}$	$(1 + 4Fo(1 + Bi))T_{m,n}^{p+1} - 2Fo(T_{m-1,n}^{p+1} + T_{m,n-1}^{p+1} + 2Bi T_{\infty}) = T_{m,n}^p + 4Bi Fo T_{\infty}$	$(5.89)$ $(5.97)$
	4. Node at exterior corner with convection			

<sup>a</sup>To obtain the finite-difference equation and/or stability criterion for an adiabatic surface (or surface of symmetry), simply set  $Bi$  equal to zero.

**Schematic:****Assumptions:**

1. One-dimensional conduction in  $x$ .
2. Uniform generation.
3. Constant properties.

**Analysis:** A numerical solution will be obtained using a space increment of  $\Delta x = 2 \text{ mm}$ . Since there is symmetry about the midplane, the nodal network yields six unknown nodal temperatures. Using the energy balance method, Equation 5.81, an explicit finite-difference equation may be derived for any interior node  $m$ .

$$kA \frac{T_{m-1}^p - T_m^p}{\Delta x} + kA \frac{T_{m+1}^p - T_m^p}{\Delta x} + \dot{q}A \Delta x = \rho A \Delta x c \frac{T_m^{p+1} - T_m^p}{\Delta t}$$

Solving for  $T_m^{p+1}$  and rearranging,

$$T_m^{p+1} = Fo \left[ T_{m-1}^p + T_{m+1}^p + \frac{\dot{q}(\Delta x)^2}{k} \right] + (1 - 2Fo)T_m^p \quad (1)$$

This equation may be used for node 0, with  $T_{m-1}^p = T_{m+1}^p$ , as well as for nodes 1, 2, 3, and 4. Applying energy conservation to a control volume about node 5,

$$hA(T_\infty - T_5^p) + kA \frac{T_4^p - T_5^p}{\Delta x} + \dot{q}A \frac{\Delta x}{2} = \rho A \frac{\Delta x}{2} c \frac{T_5^{p+1} - T_5^p}{\Delta t}$$

or

$$T_5^{p+1} = 2Fo \left[ T_4^p + Bi T_\infty + \frac{\dot{q}(\Delta x)^2}{2k} \right] + (1 - 2Fo - 2Bi Fo)T_5^p \quad (2)$$

Since the most restrictive stability criterion is associated with Equation 2, we select  $Fo$  from the requirement that

$$Fo(1 + Bi) \leq \frac{1}{2}$$

Hence, with

$$Bi = \frac{h \Delta x}{k} = \frac{1100 \text{ W/m}^2 \cdot \text{K} (0.002 \text{ m})}{30 \text{ W/m} \cdot \text{K}} = 0.0733$$

it follows that

$$Fo \leq 0.466$$

or

$$\Delta t = \frac{Fo(\Delta x)^2}{\alpha} \leq \frac{0.466(2 \times 10^{-3} \text{ m})^2}{5 \times 10^{-6} \text{ m}^2/\text{s}} \leq 0.373 \text{ s}$$

To be well within the stability limit, we select  $\Delta t = 0.3 \text{ s}$ , which corresponds to

$$Fo = \frac{5 \times 10^{-6} \text{ m}^2/\text{s}(0.3 \text{ s})}{(2 \times 10^{-3} \text{ m})^2} = 0.375$$

Substituting numerical values, including  $\dot{q} = \dot{q}_2 = 2 \times 10^7 \text{ W/m}^3$ , the nodal equations become

$$T_0^{p+1} = 0.375(2T_1^p + 2.67) + 0.250T_0^p$$

$$T_1^{p+1} = 0.375(T_0^p + T_2^p + 2.67) + 0.250T_1^p$$

$$T_2^{p+1} = 0.375(T_1^p + T_3^p + 2.67) + 0.250T_2^p$$

$$T_3^{p+1} = 0.375(T_2^p + T_4^p + 2.67) + 0.250T_3^p$$

$$T_4^{p+1} = 0.375(T_3^p + T_5^p + 2.67) + 0.250T_4^p$$

$$T_5^{p+1} = 0.750(T_4^p + 19.67) + 0.195T_5^p$$

To begin the marching solution, the initial temperature distribution must be known. This distribution is given by Equation 3.42, with  $\dot{q} = \dot{q}_1$ . Obtaining  $T_s = T_5$  from Equation 3.46,

$$T_s = T_\infty + \frac{\dot{q}L}{h} = 250^\circ\text{C} + \frac{10^7 \text{ W/m}^3 \times 0.01 \text{ m}}{1100 \text{ W/m}^2 \cdot \text{K}} = 340.91^\circ\text{C}$$

it follows that

$$T(x) = 16.67 \left( 1 - \frac{x^2}{L^2} \right) + 340.91^\circ\text{C}$$

Computed temperatures for the nodal points of interest are shown in the first row of the accompanying table.

Using the finite-difference equations, the nodal temperatures may be sequentially calculated with a time increment of 0.3 s until the desired final time is reached. The results are illustrated in rows 2 through 6 of the table and may be contrasted

with the new steady-state condition (row 7), which was obtained by using Equations 3.42 and 3.46 with  $\dot{q} = \dot{q}_2$ :

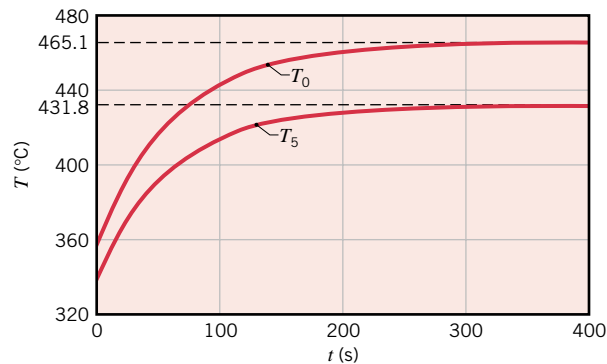
**Tabulated Nodal Temperatures**

$p$	$t(\text{s})$	$T_0$	$T_1$	$T_2$	$T_3$	$T_4$	$T_5$
0	0	357.58	356.91	354.91	351.58	346.91	340.91
1	0.3	358.08	357.41	355.41	352.08	347.41	341.41
2	0.6	358.58	357.91	355.91	352.58	347.91	341.88
3	0.9	359.08	358.41	356.41	353.08	348.41	342.35
4	1.2	359.58	358.91	356.91	353.58	348.89	342.82
5	1.5	360.08	359.41	357.41	354.07	349.37	343.27
$\infty$	$\infty$	465.15	463.82	459.82	453.15	443.82	431.82

**Comments:**

1. It is evident that at 1.5 s, the wall is in the early stages of the transient process and that many additional calculations would have to be made to reach steady-state conditions with the finite-difference solution. The computation time could be reduced slightly by using the maximum allowable time increment ( $\Delta t = 0.373$  s), but with some loss of accuracy. In the interest of maximizing accuracy, the time interval should be reduced until the computed results become independent of further reductions in  $\Delta t$ .

Extending the finite-difference solution, the time required to achieve the new steady-state condition may be determined, with temperature histories computed for the midplane (0) and surface (5) nodes having the following forms:



With steady-state temperatures of  $T_0 = 465.15^\circ\text{C}$  and  $T_5 = 431.82^\circ\text{C}$ , it is evident that the new equilibrium condition is reached within 250 s of the step change in operating power.

2. The *IHT* option entitled *Tools, Finite-Difference Equations, One-Dimensional, Transient* can be used to express the nodal equations according to the implicit method of solution. In solving the equations, the user is prompted to enter the initial temperature of each node on the *Initial Condition (IC)* pad. The problem may also be solved using *FEHT*, with the initial temperature distribution determined by applying the *Steady-State* command of the *Set-up* menu for

$\dot{q}_1 = 10^7 \text{ W/m}^3$ . The generation rate may then be changed to  $\dot{q}_2 = 2 \times 10^7 \text{ W/m}^3$ , and after enabling the *Transient* command of the *Set-up* menu, the *Continue* command of the *Solve* menu may be activated to obtain the transient solution. For details on application of *IHT* or *FEHT* to transient conduction problems, refer to the booklet *Software Tools and User's Guides*, which accompanies the software.

### 5.10.2 Discretization of the Heat Equation: The Implicit Method

In the *explicit* finite-difference scheme, the temperature of any node at  $t + \Delta t$  may be calculated from knowledge of temperatures at the same and neighboring nodes for the *preceding time*  $t$ . Hence determination of a nodal temperature at some time is *independent* of temperatures at other nodes for the *same time*. Although the method offers computational convenience, it suffers from limitations on the selection of  $\Delta t$ . For a given space increment, the time interval must be compatible with stability requirements. Frequently, this dictates the use of extremely small values of  $\Delta t$ , and a very large number of time intervals may be necessary to obtain a solution.

A reduction in the amount of computation time may often be realized by employing an *implicit*, rather than explicit, finite-difference scheme. The implicit form of a finite-difference equation may be derived by using Equation 5.74 to approximate the time derivative, while evaluating all other temperatures at the *new* ( $p + 1$ ) time, instead of the previous ( $p$ ) time. Equation 5.74 is then considered to provide a *backward-difference* approximation to the time derivative. In contrast to Equation 5.75, the implicit form of the finite-difference equation for the interior node of a two-dimensional system is then

$$\frac{1}{\alpha} \frac{T_{m,n}^{p+1} - T_{m,n}^p}{\Delta t} = \frac{T_{m+1,n}^{p+1} + T_{m-1,n}^{p+1} - 2T_{m,n}^{p+1}}{(\Delta x)^2} + \frac{T_{m,n+1}^{p+1} + T_{m,n-1}^{p+1} - 2T_{m,n}^{p+1}}{(\Delta y)^2} \quad (5.91)$$

Rearranging and assuming  $\Delta x = \Delta y$ , it follows that

$$(1 + 4Fo)T_{m,n}^{p+1} - Fo(T_{m+1,n}^{p+1} + T_{m-1,n}^{p+1} + T_{m,n+1}^{p+1} + T_{m,n-1}^{p+1}) = T_{m,n}^p \quad (5.92)$$

From Equation 5.92 it is evident that the *new* temperature of the  $m, n$  node depends on the *new* temperatures of its adjoining nodes, which are, in general, unknown. Hence, to determine the unknown nodal temperatures at  $t + \Delta t$ , the corresponding nodal equations must be *solved simultaneously*. Such a solution may be effected by using Gauss–Seidel iteration or matrix inversion, as discussed in Section 4.5. The *marching solution* would then involve simultaneously solving the nodal equations at each time  $t = \Delta t, 2\Delta t, \dots$ , until the desired final time was reached.

Relative to the explicit method, the implicit formulation has the important advantage of being *unconditionally stable*. That is, the solution remains stable for all space and time intervals, in which case there are no restrictions on  $\Delta x$  and  $\Delta t$ .



Since larger values of  $\Delta t$  may therefore be used with an implicit method, computation times may often be reduced, with little loss of accuracy. Nevertheless, to maximize accuracy,  $\Delta t$  should be sufficiently small to ensure that the results are independent of further reductions in its value.

The implicit form of a finite-difference equation may also be derived from the energy balance method. For the surface node of Figure 5.12, it is readily shown that

$$(1 + 2Fo + 2Fo Bi)T_0^{p+1} - 2Fo T_1^{p+1} = 2Fo Bi T_\infty + T_0^p \quad (5.93)$$

For any interior node of Figure 5.12, it may also be shown that

$$(1 + 2Fo)T_m^{p+1} - Fo (T_{m-1}^{p+1} + T_{m+1}^{p+1}) = T_m^p \quad (5.94)$$

Forms of the implicit finite-difference equation for other common geometries are presented in Table 5.3(b). Each equation may be derived by applying the energy balance method.

### EXAMPLE 5.10

A thick slab of copper initially at a uniform temperature of  $20^\circ\text{C}$  is suddenly exposed to radiation at one surface such that the net heat flux is maintained at a constant value of  $3 \times 10^5 \text{ W/m}^2$ . Using the explicit and implicit finite-difference techniques with a space increment of  $\Delta x = 75 \text{ mm}$ , determine the temperature at the irradiated surface and at an interior point that is  $150 \text{ mm}$  from the surface after  $2 \text{ min}$  have elapsed. Compare the results with those obtained from an appropriate analytical solution.

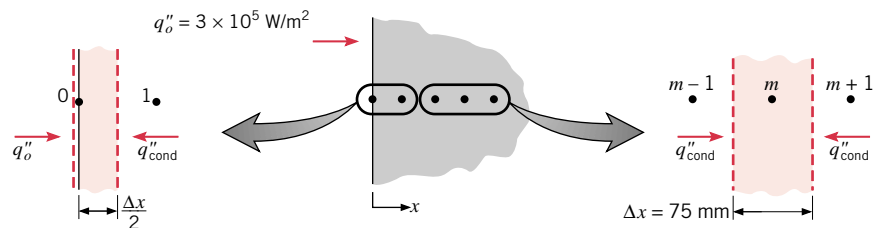
### SOLUTION

**Known:** Thick slab of copper, initially at a uniform temperature, is subjected to a constant net heat flux at one surface.

### Find:

1. Using the explicit finite-difference method, determine temperatures at the surface and  $150 \text{ mm}$  from the surface after an elapsed time of  $2 \text{ min}$ .
2. Repeat the calculations using the implicit finite-difference method.
3. Determine the same temperatures analytically.

### Schematic:



**Assumptions:**

1. One-dimensional conduction in  $x$ .
2. Thick slab may be approximated as a semi-infinite medium with constant surface heat flux.
3. Constant properties.

**Properties:** Table A.1, copper (300 K):  $k = 401 \text{ W/m} \cdot \text{K}$ ,  $\alpha = 117 \times 10^{-6} \text{ m}^2/\text{s}$ .

**Analysis:**

1. An explicit form of the finite-difference equation for the surface node may be obtained by applying an energy balance to a control volume about the node.

$$q_o'' A + kA \frac{T_1^p - T_0^p}{\Delta x} = \rho A \frac{\Delta x}{2} c \frac{T_0^{p+1} - T_0^p}{\Delta t}$$

or

$$T_0^{p+1} = 2Fo \left( \frac{q_o'' \Delta x}{k} + T_1^p \right) + (1 - 2Fo) T_0^p$$

The finite-difference equation for any interior node is given by Equation 5.78. Both the surface and interior nodes are governed by the stability criterion

$$Fo \leq \frac{1}{2}$$

Noting that the finite-difference equations are simplified by choosing the maximum allowable value of  $Fo$ , we select  $Fo = \frac{1}{2}$ . Hence

$$\Delta t = Fo \frac{(\Delta x)^2}{\alpha} = \frac{1}{2} \frac{(0.075 \text{ m})^2}{117 \times 10^{-6} \text{ m}^2/\text{s}} = 24 \text{ s}$$

With

$$\frac{q_o'' \Delta x}{k} = \frac{3 \times 10^5 \text{ W/m}^2 (0.075 \text{ m})}{401 \text{ W/m} \cdot \text{K}} = 56.1^\circ\text{C}$$

the finite-difference equations become

$$T_0^{p+1} = 56.1^\circ\text{C} + T_1^p \quad \text{and} \quad T_m^{p+1} = \frac{T_{m+1}^p + T_{m-1}^p}{2}$$

for the surface and interior nodes, respectively. Performing the calculations, the results are tabulated as follows:

**Explicit Finite-Difference Solution for  $Fo = \frac{1}{2}$** 

$p$	$t(\text{s})$	$T_0$	$T_1$	$T_2$	$T_3$	$T_4$
0	0	20	20	20	20	20
1	24	76.1	20	20	20	20
2	48	76.1	48.1	20	20	20
3	72	104.2	48.1	34.1	20	20
4	96	104.2	69.1	34.1	27.1	20
5	120	125.3	69.1	48.1	27.1	20

After 2 min, the surface temperature and the desired interior temperature are  $T_0 = 125.3^\circ\text{C}$  and  $T_2 = 48.1^\circ\text{C}$ .

Note that calculation of identical temperatures at successive times for the same node is an idiosyncrasy of using the maximum allowable value of  $Fo$  with the explicit finite-difference technique. The actual physical condition is, of course, one in which the temperature changes continuously with time. The idiosyncrasy is eliminated and the accuracy of the calculations is improved by reducing the value of  $Fo$ .

To determine the extent to which the accuracy may be improved by reducing  $Fo$ , let us redo the calculations for  $Fo = \frac{1}{4}(\Delta t = 12 \text{ s})$ . The finite-difference equations are then of the form

$$T_0^{p+1} = \frac{1}{2}(56.1^\circ\text{C} + T_1^p) + \frac{1}{2}T_0^p$$

$$T_m^{p+1} = \frac{1}{4}(T_{m+1}^p + T_{m-1}^p) + \frac{1}{2}T_m^p$$

and the results of the calculations are tabulated as follows:

**Explicit Finite-Difference Solution for  $Fo = \frac{1}{4}$**

$p$	$t(\text{s})$	$T_0$	$T_1$	$T_2$	$T_3$	$T_4$	$T_5$	$T_6$	$T_7$	$T_8$
0	0	20	20	20	20	20	20	20	20	20
1	12	48.1	20	20	20	20	20	20	20	20
2	24	62.1	27.0	20	20	20	20	20	20	20
3	36	72.6	34.0	21.8	20	20	20	20	20	20
4	48	81.4	40.6	24.4	20.4	20	20	20	20	20
5	60	89.0	46.7	27.5	21.3	20.1	20	20	20	20
6	72	95.9	52.5	30.7	22.6	20.4	20.0	20	20	20
7	84	102.3	57.9	34.1	24.1	20.8	20.1	20.0	20	20
8	96	108.1	63.1	37.6	25.8	21.5	20.3	20.0	20.0	20
9	108	113.7	68.0	41.0	27.6	22.2	20.5	20.1	20.0	20.0
10	120	118.9	72.6	44.4	29.6	23.2	20.8	20.2	20.0	20.0

After 2 min, the desired temperatures are  $T_0 = 118.9^\circ\text{C}$  and  $T_2 = 44.4^\circ\text{C}$ . Comparing the above results with those obtained for  $Fo = \frac{1}{2}$ , it is clear that by reducing  $Fo$  we have eliminated the problem of recurring temperatures. We have also predicted greater thermal penetration (to node 6 instead of node 3). An assessment of the improvement in accuracy must await a comparison with results based on an exact solution.

2. Performing an energy balance on a control volume about the surface node, the implicit form of the finite-difference equation is

$$q_o'' + k \frac{T_1^{p+1} - T_0^{p+1}}{\Delta x} = \rho \frac{\Delta x}{2} c \frac{T_0^{p+1} - T_0^p}{\Delta t}$$

or

$$(1 + 2Fo)T_0^{p+1} - 2FoT_1^{p+1} = \frac{2\alpha q_o'' \Delta t}{k \Delta x} + T_0^p$$

Arbitrarily choosing  $Fo = \frac{1}{2}(\Delta t = 24 \text{ s})$ , it follows that

$$2T_0^{p+1} - T_1^{p+1} = 56.1 + T_0^p$$

From Equation 5.94, the finite-difference equation for any interior node is then of the form

$$-T_{m-1}^{p+1} + 4T_m^{p+1} - T_{m+1}^{p+1} = 2T_m^p$$

Since we are dealing with a semi-infinite solid, the number of nodes is, in principle, infinite. In practice, however, the number may be limited to the nodes that are affected by the change in the boundary condition for the time of interest. From the results of the explicit method, it is evident that we are safe in choosing nine nodes corresponding to  $T_0, T_1, \dots, T_8$ . We are thereby assuming that, at  $t = 120$  s, there has been no change in  $T_8$ .

We now have a set of nine equations that must be solved simultaneously for each time increment. Using the matrix inversion method, we express the equations in the form  $[A][T] = [C]$ , where

$$[A] = \begin{bmatrix} 2 & -1 & 0 & 0 & 0 & 0 & 0 & 0 & 0 \\ -1 & 4 & -1 & 0 & 0 & 0 & 0 & 0 & 0 \\ 0 & -1 & 4 & -1 & 0 & 0 & 0 & 0 & 0 \\ 0 & 0 & -1 & 4 & -1 & 0 & 0 & 0 & 0 \\ 0 & 0 & 0 & -1 & 4 & -1 & 0 & 0 & 0 \\ 0 & 0 & 0 & 0 & -1 & 4 & -1 & 0 & 0 \\ 0 & 0 & 0 & 0 & 0 & -1 & 4 & -1 & 0 \\ 0 & 0 & 0 & 0 & 0 & 0 & -1 & 4 & -1 \\ 0 & 0 & 0 & 0 & 0 & 0 & 0 & -1 & 4 \end{bmatrix}$$

$$[C] = \begin{bmatrix} 56.1 + T_0^p \\ 2T_1^p \\ 2T_2^p \\ 2T_3^p \\ 2T_4^p \\ 2T_5^p \\ 2T_6^p \\ 2T_7^p \\ 2T_8^p + T_9^{p+1} \end{bmatrix}$$

Note that numerical values for the components of  $[C]$  are determined from previous values of the nodal temperatures. Note also how the finite-difference equation for node 8 appears in matrices  $[A]$  and  $[C]$ .

A table of nodal temperatures may be compiled, beginning with the first row ( $p = 0$ ) corresponding to the prescribed initial condition. To obtain nodal temperatures for subsequent times, the inverse of the coefficient matrix  $[A]^{-1}$  must first be found. At each time  $p + 1$ , it is then multiplied by the column vector  $[C]$ , which is evaluated at  $p$ , to obtain the temperatures  $T_0^{p+1}, T_1^{p+1}, \dots, T_8^{p+1}$ . For example, multiplying  $[A]^{-1}$  by the column vector corresponding to  $p = 0$ ,

$$[C]_{p=0} = \begin{bmatrix} 76.1 \\ 40 \\ 40 \\ 40 \\ 40 \\ 40 \\ 40 \\ 40 \\ 60 \end{bmatrix}$$

the second row of the table is obtained. Updating  $[C]$ , the process is repeated four more times to determine the nodal temperatures at 120 s. The desired temperatures are  $T_0 = 114.7^\circ\text{C}$  and  $T_2 = 44.2^\circ\text{C}$ .

#### Implicit Finite-Difference Solution for $Fo = \frac{1}{2}$

$p$	$t(\text{s})$	$T_0$	$T_1$	$T_2$	$T_3$	$T_4$	$T_5$	$T_6$	$T_7$	$T_8$
0	0	20.0	20.0	20.0	20.0	20.0	20.0	20.0	20.0	20.0
1	24	52.4	28.7	22.3	20.6	20.2	20.0	20.0	20.0	20.0
2	48	74.0	39.5	26.6	22.1	20.7	20.2	20.1	20.0	20.0
3	72	90.2	50.3	32.0	24.4	21.6	20.6	20.2	20.1	20.0
4	96	103.4	60.5	38.0	27.4	22.9	21.1	20.4	20.2	20.1
5	120	114.7	70.0	44.2	30.9	24.7	21.9	20.8	20.3	20.1

3. Approximating the slab as a semi-infinite medium, the appropriate analytical expression is given by Equation 5.59, which may be applied to any point in the slab.

$$T(x, t) - T_i = \frac{2q_o''(\alpha t/\pi)^{1/2}}{k} \exp\left(-\frac{x^2}{4\alpha t}\right) - \frac{q_o''x}{k} \operatorname{erfc}\left(\frac{x}{2\sqrt{\alpha t}}\right)$$

At the surface, this expression yields

$$T(0, 120 \text{ s}) - 20^\circ\text{C} = \frac{2 \times 3 \times 10^5 \text{ W/m}^2}{401 \text{ W/m} \cdot \text{K}} (117 \times 10^{-6} \text{ m}^2/\text{s} \times 120 \text{ s}/\pi)^{1/2}$$

or

$$T(0, 120 \text{ s}) = 120.0^\circ\text{C}$$

At the interior point ( $x = 0.15 \text{ m}$ )

$$\begin{aligned} T(0.15 \text{ m}, 120 \text{ s}) - 20^\circ\text{C} &= \frac{2 \times 3 \times 10^5 \text{ W/m}^2}{401 \text{ W/m} \cdot \text{K}} \\ &\times (117 \times 10^{-6} \text{ m}^2/\text{s} \times 120 \text{ s}/\pi)^{1/2} \\ &\times \exp\left[-\frac{(0.15 \text{ m})^2}{4 \times 117 \times 10^{-6} \text{ m}^2/\text{s} \times 120 \text{ s}}\right] \\ &- \frac{3 \times 10^5 \text{ W/m}^2 \times 0.15 \text{ m}}{401 \text{ W/m} \cdot \text{K}} \\ &\times \left[1 - \operatorname{erf}\left(\frac{0.15 \text{ m}}{2\sqrt{117 \times 10^{-6} \text{ m}^2/\text{s} \times 120 \text{ s}}}\right)\right] \\ T(0.15 \text{ m}, 120 \text{ s}) &= 45.4^\circ\text{C} \end{aligned}$$

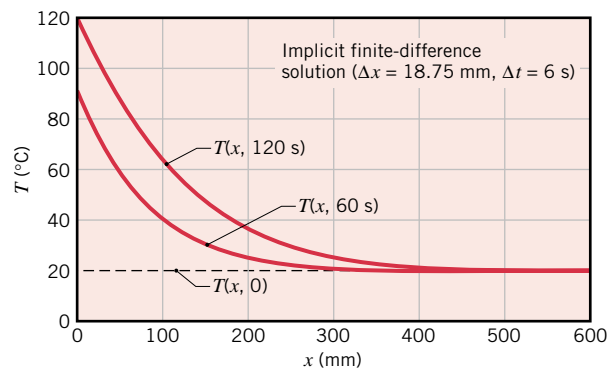
#### Comments:

1. Comparing the exact results with those obtained from the three approximate solutions, it is clear that the explicit method with  $Fo = \frac{1}{4}$  provides the most accurate predictions.

Method	$T_0 = T(0, 120 \text{ s})$	$T_2 = T(0.15 \text{ m}, 120 \text{ s})$
Explicit ( $Fo = \frac{1}{2}$ )	125.3	48.1
Explicit ( $Fo = \frac{1}{4}$ )	118.9	44.4
Implicit ( $Fo = \frac{1}{2}$ )	114.7	44.2
Exact	120.0	45.4

This is not unexpected, since the corresponding value of  $\Delta t$  is 50% smaller than that used in the other two methods. Although computations are simplified by using the maximum allowable value of  $Fo$  in the explicit method, the accuracy of the results is seldom satisfactory.

- The accuracy of the foregoing calculations is adversely affected by the coarse grid ( $\Delta x = 75 \text{ mm}$ ), as well as by the large time steps ( $\Delta t = 24 \text{ s}, 12 \text{ s}$ ). Applying the implicit method with  $\Delta x = 18.75 \text{ mm}$  and  $\Delta t = 6 \text{ s}$  ( $Fo = 2.0$ ), the solution yields  $T_0 = T(0, 120 \text{ s}) = 119.2^\circ\text{C}$  and  $T_2 = T(0.15 \text{ m}, 120 \text{ s}) = 45.3^\circ\text{C}$ , both of which are in good agreement with the exact solution. Complete temperature distributions may be plotted at any of the discrete times, and results obtained at  $t = 60$  and  $120 \text{ s}$  are as follows:



Note that, at  $t = 120 \text{ s}$ , the assumption of a semi-infinite medium would remain valid if the thickness of the slab exceeded approximately  $500 \text{ mm}$ .

- Note that the coefficient matrix  $[A]$  is *tridiagonal*. That is, all elements are zero except those that are on, or to either side of, the main diagonal. Tridiagonal matrices are associated with one-dimensional conduction problems.
- A more general radiative heating condition would be one in which the surface is suddenly exposed to large surroundings at an elevated temperature  $T_{\text{sur}}$  (Problem 5.107). The net rate at which radiation is transferred to the surface may then be calculated from Equation 1.7. Allowing for convection heat transfer to the surface, application of conservation of energy to the surface node yields an explicit finite-difference equation of the form

$$\varepsilon\sigma[T_{\text{sur}}^4 - (T_0^p)^4] + h(T_{\infty} - T_0^p) + k \frac{T_1^p - T_0^p}{\Delta x} = \rho \frac{\Delta x}{2} c \frac{T_0^{p+1} - T_0^p}{\Delta t}$$

Use of this finite-difference equation in a numerical solution is complicated by the fact that it is *nonlinear*. However, the equation may be *linearized* by introducing

the radiation heat transfer coefficient  $h_r$ , defined by Equation 1.9, and the finite-difference equation is

$$h_r^p(T_{\text{sur}} - T_0^p) + h(T_\infty - T_0^p) + k \frac{T_1^p - T_0^p}{\Delta x} = \rho \frac{\Delta x}{2} c \frac{T_0^{p+1} - T_0^p}{\Delta t}$$

The solution may proceed in the usual manner, although the effect of a radiative Biot number ( $Bi_r \equiv h_r \Delta x/k$ ) must be included in the stability criterion and the value of  $h_r$  must be updated at each step in the calculations. If the implicit method is used,  $h_r$  is calculated at  $p + 1$ , in which case an iterative calculation must be made at each time step.

5. The *IHT Tools, Finite-Difference Equations, One-Dimensional, Transient* option can be used to formulate the nodal equations for the implicit method. A schematic of the pertinent node and its control volume appears in the tool pad, with provision for entering indices associated with the node of interest and relevant adjoining nodes. The system of equations, with comments, has this form:

```
//Node 0

rho * cp * der(T0,t) = fd_1d_sur_w(T0,T1,k,qdot,deltax,Tinf,h,q''a0)
q''a0 = 3e5           // Applied heat flux, W/m^2
Tinf = 20            // Arbitrary value for convection process
h = 1e-20            // Makes convection process negligible

// Interior nodes, 1 - 8
rho*cp*der(T1,t) = fd_1d_int(T1,T2,T0,k,qdot,deltax)
rho*cp*der(T2,t) = fd_1d_int(T2,T3,T1,k,qdot,deltax)
rho*cp*der(T3,t) = fd_1d_int(T3,T4,T2,k,qdot,deltax)
rho*cp*der(T4,t) = fd_1d_int(T4,T5,T3,k,qdot,deltax)
rho*cp*der(T5,t) = fd_1d_int(T5,T6,T4,k,qdot,deltax)
rho*cp*der(T6,t) = fd_1d_int(T6,T7,T5,k,qdot,deltax)
rho*cp*der(T7,t) = fd_1d_int(T7,T8,T6,k,qdot,deltax)
rho*cp*der(T8,t) = fd_1d_int(T8,T9,T7,k,qdot,deltax)
```

Note that the prescribed convection coefficient renders convection negligible, as required by the problem statement. Using  $\Delta x = 75$  mm and  $\Delta t = 12$  s, the solution yields  $T_0 = T(0,120 \text{ s}) = 116.0^\circ\text{C}$  and  $T_2 = T(150 \text{ mm}, 120 \text{ s}) = 44.2^\circ\text{C}$ . Contrast these results with those summarized in Comment 1.

6. This example is provided in *FEHT* as a solved model accessed through the *Tool-bar* menu, *Examples*. The input screen summarizes key pre- and post-processing steps, as well as results for nodal spacings of 1 and 0.125 mm. As an exercise, press *Run* to solve for the nodal temperatures, and in the *View* menu, select *Temperature Contours* to represent the temperature field in the form of isotherms.

## 5.11

### Summary

Transient conduction occurs in numerous engineering applications and may be treated using different methods. There is certainly much to be said for simplicity, in which case, when confronted with a transient problem, the first thing you should do

is calculate the Biot number. If this number is much less than unity, you may use the lumped capacitance method to obtain accurate results with minimal computational requirements. However, if the Biot number is not much less than unity, spatial effects must be considered, and some other method must be used. Analytical results are available in convenient graphical and equation form for the plane wall, the infinite cylinder, the sphere, and the semi-infinite solid. You should know when and how to use these results. If geometrical complexities and/or the form of the boundary conditions preclude their use, recourse must be made to an approximate numerical technique, such as the finite-difference method.

You may test your understanding of key concepts by addressing the following questions.

- Under what conditions may the *lumped capacitance method* be used to predict the transient response of a solid to a change in its thermal environment?
- What is the physical interpretation of the *Biot number*?
- Is the lumped capacitance method of analysis likely to be more applicable for a hot solid being cooled by forced convection in air or in water? By forced convection in air or natural convection in air?
- Is the lumped capacitance method of analysis likely to be more applicable for cooling of a hot solid made of copper or aluminum? For silicon nitride or glass?
- What parameters determine the *time constant* associated with the transient thermal response of a lumped capacitance solid? Is this response accelerated or decelerated by an increase in the convection coefficient? By an increase in the density or specific heat of the solid?
- For one-dimensional, transient conduction in a plane wall, a long cylinder or a sphere with surface convection, what dimensionless parameters may be used to simplify the representation of thermal conditions? How are these parameters defined?
- Why is the semi-infinite solution applicable to any geometry at early times?
- What is the physical interpretation of the *Fourier number*?
- What requirement must be satisfied for use of a *one-term approximation* to determine the transient thermal response of a plane wall, a long cylinder or a sphere experiencing one-dimensional conduction due to a change in surface conditions? At what stage of a transient process is the requirement not satisfied?
- What does transient heating or cooling of a plane wall with equivalent convection conditions at opposite surfaces have in common with a plane wall heated or cooled by convection at one surface and well insulated at the other surface?
- How may a one-term approximation be used to determine the transient thermal response of a plane wall, long cylinder, or sphere subjected to a sudden change in surface temperature?
- For one-dimensional, transient conduction, what is implied by the idealization of a *semi-infinite* solid? Under what conditions may the idealization be applied to a plane wall?
- What differentiates an *explicit*, finite-difference solution to a transient conduction problem from an *implicit* solution?
- What is meant by characterization of the implicit finite-difference method as *unconditionally stable*? What constraint is placed on the explicit method to ensure a stable solution?



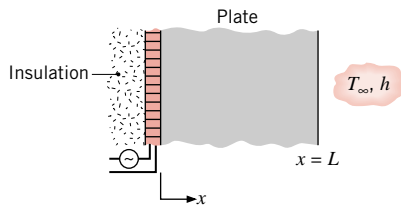
## References

1. Carslaw, H. S., and J. C. Jaeger, *Conduction of Heat in Solids*, 2nd ed., Oxford University Press, London, 1986.
2. Schneider, P. J., *Conduction Heat Transfer*, Addison-Wesley, Reading, MA, 1957.
3. Kakac, S., and Y. Yener, *Heat Conduction*, Taylor & Francis, Washington, DC, 1993.
4. Poulidakos, D., *Conduction Heat Transfer*, Prentice-Hall, Englewood Cliffs, NJ, 1994.
5. Yovanovich, M. M., "Conduction and Thermal Contact Resistances (Conductances)," in W. M. Rohsenow, J. P. Hartnett, and Y. I. Cho, Eds. *Handbook of Heat Transfer*, McGraw-Hill, New York, 1998, pp. 3.1–3.73.
6. Hirsch, L. R., R. J. Stafford, J. A. Bankson, S. R. Serksen, B. Rivera, R. E. Price, J. D. Hazle, N. J. Halas, and J. L. West, *Proc. Nat. Acad. Sciences of the U.S.*, **100**, 13549–13554, 2003.
7. Cahill, D.G., *Rev. Sci. Instrum.*, **61**, 802–808, 1990.

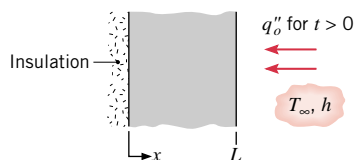
## Problems

### Qualitative Considerations

- 5.1 Consider a thin electrical heater attached to a plate and backed by insulation. Initially, the heater and plate are at the temperature of the ambient air,  $T_\infty$ . Suddenly, the power to the heater is activated, yielding a constant heat flux  $q_o''$  (W/m<sup>2</sup>) at the inner surface of the plate.



- (a) Sketch and label, on  $T$ - $x$  coordinates, the temperature distributions: initial, steady-state, and at two intermediate times.
  - (b) Sketch the heat flux at the outer surface  $q_x''(L, t)$  as a function of time.
- 5.2 The inner surface of a plane wall is insulated while the outer surface is exposed to an airstream at  $T_\infty$ . The wall is at a uniform temperature corresponding to that of the airstream. Suddenly, a radiation heat source is switched on applying a uniform flux  $q_o''$  to the outer surface.



- (a) Sketch and label, on  $T$ - $x$  coordinates, the temperature distributions: initial, steady-state, and at two intermediate times.

- (b) Sketch the heat flux at the outer surface  $q_x''(L, t)$  as a function of time.

- 5.3 A microwave oven operates on the principle that application of a high-frequency field causes electrically polarized molecules in food to oscillate. The net effect is a nearly *uniform generation* of thermal energy within the food. Consider the process of cooking a slab of beef of thickness  $2L$  in a microwave oven and compare it with cooking in a conventional oven, where *each side* of the slab is *heated by radiation*. In each case the meat is to be heated from  $0^\circ\text{C}$  to a *minimum* temperature of  $90^\circ\text{C}$ . Base your comparison on a sketch of the temperature distribution at selected times for each of the cooking processes. In particular, consider the time  $t_0$  at which heating is initiated, a time  $t_1$  during the heating process, the time  $t_2$  corresponding to the conclusion of heating, and a time  $t_3$  well into the subsequent cooling process.

- 5.4 A plate of thickness  $2L$ , surface area  $A_s$ , mass  $M$ , and specific heat  $c_p$ , initially at a uniform temperature  $T_i$ , is suddenly heated on both surfaces by a convection process ( $T_\infty, h$ ) for a period of time  $t_o$ , following which the plate is insulated. Assume that the midplane temperature does not reach  $T_\infty$  within this period of time.

- (a) Assuming  $Bi \gg 1$  for the heating process, sketch and label, on  $T$ - $x$  coordinates, the following temperature distributions: initial, steady-state ( $t \rightarrow \infty$ ),  $T(x, t_o)$ , and at two intermediate times between  $t = t_o$  and  $t \rightarrow \infty$ .
- (b) Sketch and label, on  $T$ - $t$  coordinates, the midplane and exposed surface temperature distributions.
- (c) Repeat parts (a) and (b) assuming  $Bi \ll 1$  for the plate.